Optimal absorption of acoustical waves by a boundary

Thi Phuong Kieu Nguyen, Frédéric Magoulès, Pascal Omnes, Anna Rozanova-Pierrat

Optimal absorption of acoustic waves by a boundary

Frédéric Magoulès* Thi Phuong Kieu Nguyen† Pascal Omnes‡
Anna Rozanova-Pierrat§

Abstract

In the aim to find the simplest and most efficient shape of a noise absorbing wall to dissipate the acoustical energy of a sound wave, we consider a frequency model described by the Helmholtz equation with a damping on the boundary. The well-posedness of the model is shown in the most irregular possible class of d-set boundaries. For the case of a regular boundary, we prove existence of an optimal shape and provide the shape derivative of an objective function, chosen to describe the acoustic energy. For a fixed porous material, considered as an acoustic absorbent, we derive the damping boundary parameters from the corresponding time-dependent problem, described by the damped wave equation (damping in volume). Using the gradient method for the shape derivative, combined with the finite volume and level set methods, we numerically find optimal shapes for a fixed frequency and an efficient shape in a whole range of frequencies.

Keywords: Absorbing wall; wave propagation; shape optimization; Helmholtz equation; sound absorption; Robin boundary condition.

1 Introduction

The diffraction and absorption of waves by a system with both absorbing properties and irregular geometry is an open physical problem. This has to be solved to understand why anechoic chambers (electromagnetic or acoustic) do work better with irregular absorbing walls. The first studies relating irregular geometry and absorption are performed numerically in [22]. Therefore there is a question about the existence of an optimal shape of an absorbent wall (for a fixed absorbing material), optimal in the sense that it is as dissipative as possible for a large range of frequencies, and at the same time that such a wall could effectively be constructed. In the framework of the propagation of acoustic waves, the acoustic absorbent material of the wall is considered as a porous medium. In this article, for a fixed frequency of the sound wave, we solve the shape optimization problem that consists in minimizing the acoustic energy for a frequency model with a damping on the boundary. Then we extend this method in order to find an efficient shape for a finite range of frequencies.

In the area of the optimization of acoustic performances of non absorbing walls, Duhamel [18, 19] studies sound propagation in a two-dimensional vertical cut of a road wall and uses genetic algorithms to obtain optimal shapes (some of them are however not connected and thus could not be easily manufactured). The author also uses a branch and bound (combinatorial optimization) type linear programming in order to optimize the sensors' position that allow an active noise control, following former work introduced by Lueg [27] in 1934. Abe et al. [1] consider a boundary elements based shape optimization of a non absorbing two-dimensional wall in the framework of a two-dimensional sound scattering problem for

*CentraleSupélec, Université Paris-Saclay, France.
†CentraleSupélec, Université Paris-Saclay, France.
‡Commissariat à l'Énergie Atomique et aux Énergies Saclay, France.
§CentraleSupélec, Université Paris-Saclay, France (correspondence, anna.rozanova-pierrat@centralesupelec.fr).

a fixed frequency (for the Helmholtz equation) using a topological derivative with the principle that a new shape or topology is obtained by nucleating small scattering bodies. Also for the Helmholtz equation for a fixed frequency, using the shape derivative of a functional representing the acoustical energy, Cao and Stanescu [10] consider a two-dimensional shape design problem for a non-absorbing part of the boundary to reduce the amount of noise radiated from aircraft turbofan engines. For the same problem, Farhadinia [21] developed a method based on measure theory, which does not require any information about gradients and the differentiability of the cost function.

On the other hand, for shape optimization problems there are theoretical results, reviewed in Refs. [4, 38], which rely on the topological derivatives of the cost functional to be minimized, with numerical application of the gradient method in both two and three dimensional cases (in the framework of solid mechanics). In particular, Achdou and Pironneau [2] considered the problem of optimization of a photocell, using a complex-valued Helmholtz problem with periodic boundary conditions with the aim to maximize the solar energy in a dissipative region. For acoustic waves in the two-dimensional case, optimization of the shape of an absorbing inclusion placed in a lossless acoustic medium was considered in Refs. [39, 40]. The considered model is the linear damped wave equation [14, 7]. Using the topology derivative approach, Münch et al. consider in [39, 40] the minimization of the acoustic energy of the solution of the damped wave equation at a given time $T > 0$ without any geometric restrictions and without the purpose of the design of an absorbent wall. See also [5] for the shape optimization of shell structure acoustics.

In this article, we study the two-dimensional shape optimization problem for a Helmholtz equation with a damping on the boundary, modeled by a complex-valued Robin boundary condition. The shape of the damping boundary is to be found, in the aim to minimize the total acoustical energy of the system. In section 2, we introduce the frequency model and its time-dependent analogue with a dissipation on the boundary. We analyze its dissipative properties and give the well-posedness results, due to [8, 23] for at least Lipschitz boundaries, but we generalize the results for the Helmholtz problem in the larger class of domains with d-set boundaries using [6] (see Appendix A). This class, named in [6] "admissible domains" and containing for instance the Von Koch fractals, is optimal (it is not possible to let the geometry be less regular) thanks to results of [28] on geometrical characterization of Sobolev-extension domains in $\mathbb{R}^n$. However, for the shape optimization problem only the Lipschitz boundary case is considered here.

We compare the frequency model with dissipation by the boundary to the corresponding model with a dissipation in the volume. Dissipation in the volume is described by a damped wave equation in which the values of the coefficients for a given porous medium are given as functions of its macroscopic parameters (as porosity, tortuosity and resistivity to the passage of air), as proposed by [29]. In particular, in Theorem 5 we propose a possible way to find the complex parameter in the Robin boundary condition of the former model that best approximates the latter. All numerical calculations, in particular in Theorem 6, are performed for a porous material named ISOREL, frequently used in building isolation (see Appendix B). In section 3, for the case of a Lipschitz boundary in the classical framework of shape optimization, for any fixed frequency we obtain the existence of an optimal shape. See also Ref. [9] for a free discontinuity approach to a class of shape optimization problems involving a Robin condition on a free boundary. For the case of a regular boundary we provide in section 4 the shape derivative of an objective functional chosen to describe the acoustical energy. Using the gradient descent method for the shape derivative, combined with the finite volume and level set methods introduced in section 5, we find numerically optimal shapes for a fixed frequency. In section 6, we show the stability of the numerical algorithm and the non-uniqueness of the optimal shape, which can be explained by the non-uniqueness of the geometry providing the same spectral properties (see [24, 26, 25]). Numerically, we show that for efficiency in the energy absorption, the shape of the wall must be related with the half wavelength of the wave created by the source and thus it is not pertinent to add much smaller geometric variations, which finally confirms the possibility

to create "not too complicated but most efficient" walls. At the same time, the multi-scale nature of the wall geometry is necessary for an efficient absorption in a large band of frequencies.

2 The model: motivation and known properties

To describe the acoustic wave absorption by a porous medium, there are two possibilities. The first one is to consider wave propagation in two media, typically air and a wall, which corresponds to a damping in the volume. The most common mathematical model for this is the damped wave equation [7]. The second one is to consider only one lossless medium, air, and to model energy dissipation by a damping condition on the boundary. In both cases, we need to ensure the same order of energy damping corresponding to the physical characteristics of the chosen porous medium as its porosity ϕ, tortuosity α_h and resistivity to the passage of air σ [29].

Thanks to Ref. [29], we can define the coefficients in the damped wave equation (damping in volume) as functions of the above mentioned characteristics. More precisely, for a regular bounded domain $\Omega \subset \mathbb{R}^2$ (for instance $\partial\Omega \in C^1$) composed of two disjoint parts $\Omega = \Omega_0 \cup \Omega_1$ of two homogeneous media, air in Ω_0 and a porous material in Ω_1, separated by an internal boundary Γ, we consider the following boundary value problem (for the pressure of the wave)

$$\begin{cases} \xi(x)\partial_t^2 u + a(x)\partial_t u - \nabla\cdot(\mu(x)\nabla u) = 0 \quad \text{in } \Omega, \\ \frac{\partial u}{\partial n}|_{\mathbb{R}_t\times\partial\Omega} \equiv 0, \quad [u]_\Gamma = [\mu\nabla u\cdot n]_\Gamma = 0, \\ u|_{t=0} = u_0 \mathbb{1}_{\Omega_0}, \quad \partial_t u|_{t=0} = u_1 \mathbb{1}_{\Omega_0}, \end{cases} \tag{1}$$

with $\xi(x) = \frac{1}{c_0^2}$, $a(x) = 0$, $\mu(x) = 1$ in air, *i.e.*, in Ω_0, and

$$\xi(x) = \frac{\phi\gamma_p}{c_0^2}, \quad a(x) = \sigma\frac{\phi^2\gamma_p}{c_0^2\rho_0\alpha_h}, \quad \mu(x) = \frac{\phi}{\alpha_h}$$

in the porous medium, *i.e.*, in Ω_1. The external boundary $\partial\Omega$ is supposed to be rigid, *i.e.*, Neumann boundary condition are applied, and on the internal boundary Γ we have no-jump conditions on u and $\mu\nabla u\cdot n$, where n denotes the normal unit vector to Γ. Here, c_0 and ρ_0 denote respectively the sound velocity and the density of air, whereas $\gamma_p = 7/5$ denotes the ratio of specific heats. But instead of energy absorption in volume, we can also consider the following frequency model of damping by the boundary. Let Ω be a connected bounded domain of $\mathbb{R}^2$ with a Lipschitz boundary $\partial\Omega$. We suppose that the boundary $\partial\Omega$ is divided into three parts $\partial\Omega = \Gamma_D \cup \Gamma_N \cup \Gamma$ (see Figure 1 for an example of Ω, chosen for the numerical calculations) and consider

$$\begin{cases} \triangle u + \omega^2 u = f(x), & x\in\Omega, \\ u = g(x) \quad \text{on } \Gamma_D, & \dfrac{\partial u}{\partial n} = 0 \quad \text{on } \Gamma_N, \quad \dfrac{\partial u}{\partial n} + \alpha(x)u = \mathrm{Tr}h(x) \quad \text{on } \Gamma, \end{cases} \tag{2}$$

where $\alpha(x)$ is a complex-valued regular function with a strictly positive real part ($\mathrm{Re}(\alpha) > 0$) and a strictly negative imaginary part ($\mathrm{Im}(\alpha) < 0$).

Remark 1. *This particular choice of the signs of the real and the imaginary parts of α are needed for the well-posedness properties [23] and the energy decay of the corresponding time-dependent problem. In addition, as the frequency $\omega > 0$ is supposed to be fixed, α can contain a dependence on ω, i.e., $\alpha \equiv \alpha(x,\omega)$.*

Problem (2) is a frequency version of the following time-dependent wave propagation

problem with $U(t,x) = e^{-i\omega t}u(x)$, considered in Ref. [8] for $g = 0$ on Γ_D:

$$\partial_t^2 U - \triangle U = -e^{-i\omega t} f(x), \tag{3}$$

$$U|_{t=0} = U_0, \quad \partial_t U|_{t=0} = U_1, \tag{4}$$

$$U|_{\Gamma_D} = g, \quad \left.\frac{\partial U}{\partial n}\right|_{\Gamma_N} = 0, \tag{5}$$

$$\frac{\partial U}{\partial n} - \frac{\mathrm{Im}(\alpha(x))}{\omega}\partial_t U + \mathrm{Re}(\alpha(x))U|_\Gamma = 0. \tag{6}$$

To show the energy decay, we follow [8] and introduce the Hilbert space $X_0(\Omega)$, defined as the Cartesian product of the set of functions $u \in H^1(\Omega)$, which vanish on Γ_D with the space $L_2(\Omega)$. The equivalent norm on $X_0(\Omega)$ is defined by

$$\|(u,v)\|^2_{X_0(\Omega)} = \int_\Omega \left(|\nabla_x u|^2 + |v|^2\right) \mathrm{d}x + \int_\Gamma \mathrm{Re}(\alpha(x))|u|^2 \mathrm{d}\sigma$$

with the corresponding inner product

$$\langle (u_1,u_2),(v_1,v_2)\rangle = \int_\Omega (\nabla_x u_1 \nabla_x v_1 + u_2 v_2)\,\mathrm{d}x + \int_\Gamma \mathrm{Re}(\alpha(x))u_1 v_1 \mathrm{d}\sigma. \tag{7}$$

The advantage of this norm is that the energy balance of the homogeneous problem (3)– (6) has the form

$$\partial_t \left(\|(U,\partial_t U)\|^2_{X_0(\Omega)}\right) = \frac{2}{\omega}\int_\Gamma \mathrm{Im}(\alpha(x))|\partial_t U|^2 \mathrm{d}s.$$

Therefore, for $\mathrm{Im}(\alpha) < 0$ on Γ, the energy decays in time. For the case of a smooth boundary $\partial\Omega$ (at least Lipschitz), we have the well-posedness of both models. Thanks to [8], for all $f \in L_2(\Omega)$, $(U_0,U_1) \in X_0(\Omega)$ there exists a unique solution $(U,U_t) \in C([0,\infty[,X_0(\Omega))$ of system (3)– (6) under the assumption that $\mathrm{Re}(\alpha(x)) > 0$ and $\mathrm{Im}(\alpha(x)) < 0$ are continuous functions.

For the frequency model (2) it is possible to generalize the weak well-posedness result in domains with Lipschitz boundaries [23] to domains with a more general class of boundaries, named Ahlfors d-regular sets or simply d-sets [31] (see Appendix A), using functional analysis tools on "admissible domains" developed in [6]. The interest of this generalization is that this class of domains is optimal in the sense that it is the largest possible class [6] which keeps the Sobolev extension operators, for instance $H^1(\Omega)$ to $H^1(\mathbb{R}^n)$, continuous.

We use, as in Ref. [6], the existence of the d-dimensional ($0 < d \leq n$, $d \in \mathbb{R}$) Hausdorff measure m_d on $\partial\Omega$ and a generalization of the usual trace theorem [31] (see Appendix A) and the Green formula [34, 6] in the sense of the Besov space $B^{2,2}_\beta(\partial\Omega)$ with $\beta = 1 - \frac{n-d}{2} > 0$ (for the definition of the Besov spaces on d-sets see Ref. [31] p.135 and Ref. [44]). Note that for $d = n-1$, one has $\beta = \frac{1}{2}$ and $B^{2,2}_{\frac{1}{2}}(\partial\Omega) = H^{\frac{1}{2}}(\partial\Omega)$ as usual in the case of a Lipschitz boundary. The space $L_2(\partial\Omega)$ is defined with respect to the measure m_d. Some main elements of functional analysis on d-sets are presented in Appendix A.

Considering the Helmholtz problem (2), we introduce the Hilbert space

$$V(\Omega) = \{u \in H^1(\Omega) |\ u = 0 \text{ on } \Gamma_D\} \tag{8}$$

equipped with the norm

$$\|u\|^2_{V(\Omega)} = \int_\Omega |\nabla u|^2 \mathrm{d}x + \int_\Gamma \mathrm{Re}(\alpha)|u|^2 \mathrm{d}m_d,$$

and obtain the following well-posedness result:

Theorem 1. *Let $\Omega \subset \mathbb{R}^n$ be a bounded admissible domain with a compact d-set boundary ($n-2 < d < n$) in the sense of Theorem 4, $\partial\Omega = \Gamma_D \cup \Gamma_N \cup \Gamma$ and $\beta = 1 - (n-d)/2 > 0$.*

Let in addition $\mathrm{Re}(\alpha(x)) > 0$, $\mathrm{Im}(\alpha(x)) < 0$ *be smooth functions (at least continuous) on* Γ. *Then for all* $f \in L_2(\Omega)$, $g \in B^{2,2}_\beta(\Gamma_D)$, $h \in V(\Omega)$, *and* $\omega > 0$ *there exists a unique solution* u *of the Helmholtz problem (2), such that* $(u - \tilde{g}) \in V(\Omega)$ *(where* $\tilde{g}$ *is a lifting in* $H^1(\Omega)$ *of the boundary data* g*) in the following sense: for all* $v \in V(\Omega)$

$$\int_\Omega \nabla u \cdot \nabla \bar{v} \mathrm{d}x - \omega^2 \int_\Omega u \bar{v} \mathrm{d}x + \int_\Gamma \alpha \,\mathrm{Tr}\, u \,\mathrm{Tr}\, \bar{v} \,\mathrm{d}m_d = -\int_\Omega f \bar{v} \mathrm{d}x + \int_\Gamma \mathrm{Tr}\, h \,\mathrm{Tr}\, \bar{v} \,\mathrm{d}m_d. \tag{9}$$

Moreover, the solution of problem (2) $u \in H^1(\Omega)$, *continuously depends on the data: there exists a constant* $C > 0$, *depending only on* α, ω *and on* $C_P(\Omega)$, *such that*

$$\|u\|_{H^1(\Omega)} \leq C \left(\|f\|_{L_2(\Omega)} + \|g\|_{B^{2,2}_\beta(\Gamma_D)} + \|h\|_{V(\Omega)} \right), \tag{10}$$

where $C_P(\Omega)$ *is the Poincaré constant associated to* Ω.

In particular, taking $g = 0$, *for all fixed* $\omega > 0$ *the operator*

$$B : L_2(\Omega) \times V(\Omega) \to V(\Omega), \text{ defined by } B(f, h) = u$$

with u, *the weak solution of (9), is a linear compact operator.*

In addition, if, for $m \in \mathbb{N}^*$, $\partial\Omega \in C^{m+2}$, $f \in H^m(\Omega)$ *and* $g \in H^{m+\frac{3}{2}}(\Gamma_D)$, *then the solution* u *belongs to* $H^{m+2}(\Omega)$.

Proof. Let us start with $g = 0$ and in addition suppose that α is a constant (the generalization for $\alpha(x)$ is straightforward). By the linearity of the Helmholtz problem (2), we set $u = u^f + u^h$, where u^f is the solution of the Helmholtz problem with $\mathrm{Tr}\, h = 0$ on Γ and u^h is the solution of the Helmholtz problem with $f = 0$.

When $h = 0$, the variational formulation for u^f becomes: for all $\phi \in V(\Omega)$

$$(u^f, \phi)_{V(\Omega)} - \omega^2 (u^f, \phi)_{L_2(\Omega)} + i \,\mathrm{Im}\, \alpha (\mathrm{Tr}\, u^f, \mathrm{Tr}\, \phi)_{L_2(\Gamma)} = -(f, \phi)_{L_2(\Omega)},$$

where we have defined the following equivalent inner product on $V(\Omega)$:

$$\forall (v, w) \in V(\Omega) \times V(\Omega) \quad (v, w)_{V(\Omega)} = (\nabla v, \nabla w)_{L_2(\Omega)} + \mathrm{Re}\, \alpha (\mathrm{Tr}\, v, \mathrm{Tr}\, w)_{L_2(\Gamma)}.$$

Hence, the Riesz representation Theorem ensures the existence of a linear bounded operator $A : L_2(\Omega) \to V(\Omega)$ such that for $v \in L_2(\Omega)$

$$\forall \phi \in V(\Omega) \quad (v, \phi)_{L_2(\Omega)} = (Av, \phi)_{V(\Omega)} \tag{11}$$

and in addition, by the Poincaré inequality,

$$\begin{aligned} \|Av\|_{V(\Omega)} &= \sup_{\|\phi\|_{V(\Omega)}=1} |(v, \phi)_{L_2(\Omega)}| \leq \sup_{\|\phi\|_{V(\Omega)}=1} \|v\|_{L_2(\Omega)} \|\phi\|_{L_2(\Omega)} \\ &\leq C_P(\Omega) \sup_{\|\phi\|_{V(\Omega)}=1} \|v\|_{L_2(\Omega)} \|\phi\|_{V(\Omega)} = C_P(\Omega) \|v\|_{L_2(\Omega)} \end{aligned}$$

ensuring that $\|A\| \leq C_P(\Omega)$.

In the same way, using the Riesz representation Theorem we also define a linear bounded operator $\hat{A} : L_2(\Gamma) \to V(\Omega)$ such that for $w \in L_2(\Gamma)$

$$\forall \phi \in V(\Omega) \quad (w, \mathrm{Tr}\, \phi)_{L_2(\Gamma)} = (\hat{A} w, \phi)_{V(\Omega)}.$$

Indeed, it is sufficient to notice that for a fixed $w \in L_2(\Gamma)$ the form $\ell : \phi \in V(\Omega) \mapsto \ell(\phi) = (w, \mathrm{Tr}\, \phi)_{L_2(\Gamma)} \in \mathbb{C}$ is linear and continuous on $V(\Omega)$:

$$\left| (w, \mathrm{Tr}\, \phi)_{L_2(\Gamma)} \right| \leq \|w\|_{L_2(\Gamma)} \|\mathrm{Tr}\, \phi\|_{L_2(\Gamma)} \leq C \|\phi\|_{V(\Omega)},$$

thanks to the continuity and the linearity of the trace from $V(\Omega)$ to $L_2(\Gamma)$. Moreover, $\|\hat{A}\| \leq C(\mathrm{Re}(\alpha))$ since

$$\begin{aligned}\|\hat{A}w\|_{V(\Omega)} &= \sup_{\|\phi\|_{V(\Omega)}=1} |(w, \operatorname{Tr}\phi)_{L_2(\Gamma)}| \leq \sup_{\|\phi\|_{V(\Omega)}=1} \|w\|_{L_2(\Gamma)} \|\operatorname{Tr}\phi\|_{L_2(\Gamma)} \\ &\leq C(\mathrm{Re}(\alpha)) \sup_{\|\phi\|_{V(\Omega)}=1} \|w\|_{L_2(\Gamma)} \|\phi\|_{V(\Omega)} = C(\mathrm{Re}(\alpha))\|w\|_{L_2(\Gamma)}.\end{aligned}$$

Thus, denoting by S the compact embedding operator of $V(\Omega)$ in $L_2(\Omega)$ (by the Poincaré inequality it holds that $\|S\| \leq C_P(\Omega)$), the variational formulation can be rewritten in the following form:

$$\forall \phi \in V(\Omega) \quad \Big((Id - \omega^2 A \circ S + i \operatorname{Im}\alpha \hat{A} \circ \operatorname{Tr}) u^f, \phi\Big)_{V(\Omega)} = (-Af, \phi)_{V(\Omega)}. \tag{12}$$

Thanks to the compactness of the trace operator $\operatorname{Tr} : V(\Omega) \to L_2(\partial\Omega)$ [6] (with $\|\operatorname{Tr}\| \leq C(\mathrm{Re}(\alpha))$), the operator $T = A \circ S - i\frac{\operatorname{Im}\alpha}{\omega^2}\hat{A} \circ \operatorname{Tr} : V(\Omega) \to V(\Omega)$ is compact as a composition of continuous and compact operators (with $\|T\| \leq C(\omega, \alpha, C_P(\Omega))$). Thanks to the Fredholm alternative, it is then sufficient to prove that for $(h, f) = (0, 0)$, then the unique solution is $u = 0$, and this will allow us to conclude to the well-posedness of (12). Setting $f = 0$ in (12), choosing $\phi = u^f$ and separating real and imaginary parts of the equality, we first obtain that $\operatorname{Tr} u^f = 0$ on Γ (since $|\operatorname{Im}\alpha| > 0$). By the Robin boundary condition on Γ, we then obtain that $\frac{\partial u}{\partial n} = 0$ on Γ (in the sense of a continuous linear functional on $B_\beta^{2,2}(\Gamma)$). Then, $u^f = 0$ in Ω follows by the uniqueness of the solution to the Cauchy problem for $\Delta + \omega^2 Id$ in the connected domain Ω with Cauchy data on Γ (see for example [16, Theorems 1.1 and 1.2], which can be directly adapted to the case of a domain Ω with a d-set boundary satisfying the conditions of Theorem 1 thanks to Theorem 4). The operator $(Id - \omega^2 T)^{-1}$ is thus well defined and is also a linear continuous operator, by the Fredholm alternative theorem. Thus, we obtain

$$\|u^f\|_{V(\Omega)} \leq \frac{\|A\|}{\|Id - \omega^2 T\|}\|f\|_{L_2(\Omega)} \leq C(\omega, \alpha, C_P(\Omega))\|f\|_{L_2(\Omega)}.$$

In the same way, when $f = 0$, the solution u^h in $V(\Omega)$ satisfies the following variational formulation:

$$\forall \phi \in V(\Omega) \quad \Big((Id - \omega^2 A \circ S + i \operatorname{Im}\alpha \hat{A} \circ \operatorname{Tr}) u^f, \phi\Big)_{V(\Omega)} = (\hat{A} \circ \operatorname{Tr} h, \phi)_{V(\Omega)}.$$

Hence, as previously, we have

$$\|u^h\|_{V(\Omega)} \leq \frac{\|\hat{A}\|\|\operatorname{Tr}\|}{\|Id - \omega^2 T\|}\|h\|_{V(\Omega)} \leq C(\omega, \alpha, C_P(\Omega))\|h\|_{V(\Omega)}.$$

Consequently, we have proved the well-posedness and estimate (10) for $g = 0$. Hence, by the standard lifting procedure [17] Theorem 4.1.5, we also have the result with $g \neq 0$.

To prove that the regularity of the boundary improves the regularity of the solution, we follow the classical approach, explained for elliptic equations in [20].

The linearity and the continuity of B are evident and equivalent to estimate (10). Let us prove that for any fixed $\omega > 0$, B is also compact (see also Ref. [6] for the real Robin boundary condition). Indeed, let $(f_j, h_j) \rightharpoonup (f, h)$ in $L_2(\Omega) \times V(\Omega)$. Taking for all $j \in \mathbb{N}$, $u_j = B(f_j, h_j)$ and $u = B(f, h)$, by the linearity and the continuity of B it follows that $u_j \overset{V(\Omega)}{\rightharpoonup} u$. Knowing in addition that $\operatorname{Tr} : V(\Omega) \to L_2(\Gamma)$ and the inclusion of $H^1(\Omega)$ in $L_2(\Omega)$ are compact (see Ref. [6]) we have that $\operatorname{Tr} u_j \to \operatorname{Tr} u$ in $L_2(\Gamma)$ and $u_j \to u$ in $L_2(\Omega)$. Choosing $v = u_j$ in the variational formulation (9) we find

$$\|u_j\|^2_{V(\Omega)} = \omega^2\|u_j\|^2_{L_2(\Omega)} - i\int_\Gamma \operatorname{Im}\alpha |\operatorname{Tr} u_j|^2 \mathrm{d}m_d - \int_\Omega f_j \overline{u}_j \mathrm{d}x + \int_\Gamma \operatorname{Tr} h_j \overline{\operatorname{Tr} u_j}\mathrm{d}m_d, \tag{13}$$

and hence,

$$\lim_{j\to+\infty} \|u_j\|^2_{V(\Omega)} = \omega^2\|u\|^2_{L_2(\Omega)} - i\int_\Gamma \mathrm{Im}\,\alpha|\,\mathrm{Tr}\,u|^2 \mathrm{d}m_d - \int_\Omega f\overline{u}\mathrm{d}x + \int_\Gamma \mathrm{Tr}\,h\overline{\mathrm{Tr}\,u}\mathrm{d}m_d$$
$$= \|u\|^2_{V(\Omega)}.$$

Having both $u_j \rightharpoonup u$ in $V(\Omega)$ and $\|u_j\|_{V(\Omega)} \to \|u\|_{V(\Omega)}$ implies that $u_j \to u$ in $V(\Omega)$ and hence B is compact. Since the norm $\|u\|^2_{V(\Omega)}$ on $V(\Omega)$ is equivalent [6] to the norm

$$\|u\|^2_J = A\|u\|^2_{L_2(\Omega)} + B\|\nabla u\|^2_{L_2(\Omega)} + C\|u\|^2_{L_2(\Gamma)},$$

the operator B is also compact with respect to this norm. □

In order to relate the model with a damping on the boundary and the model with a damping in the volume, we propose in Appendix B a new theorem to identify the parameter α in the Robin boundary condition (Theorem 5). This parameter provides the best approximation (in some error minimizing sense) of the latter model by the former, in the case of a flat boundary Γ.

3 Shape design problem

We consider the two dimensional shape design problem, which consists in optimizing the shape of Γ with the Robin dissipative condition in order to minimize the acoustic energy of the system (2). The boundaries with the Neumann and Dirichlet conditions Γ_D and Γ_N are supposed to be fixed.

We also define a fixed open set D with a Lipschitz boundary which contains all domains Ω.

Actually, as only a part of the boundary (precisely Γ) changes its shape, we can also impose that the changing part always lies inside of the closure of a fixed open set G with a Lipschitz boundary: $\Gamma \subset \overline{G}$. The set G forbids Γ to be too close to Γ_D, making the idea of

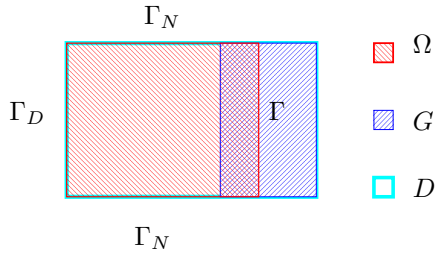

Figure 1: Example of a domain Ω in $\mathbb{R}^2$ with three types of boundaries: Γ_D and Γ_N are fixed and Γ can be changed in the restricted area $\overline{G}$. Here $\Omega \cup G = D$ and obviously $\Omega \subset D$.

an acoustical wall more realistic.

To introduce the class of admissible domains, on which we minimize the acoustical energy of system (2), we define $\mathcal{L}ip$ as the class of all domains $\Omega \subset D$ with Lipschitz boundaries of bounded length, *i.e.* we fix $M > 0$ such that for all $\Omega \in \mathcal{L}ip$ it holds $\mathrm{Vol}(\partial\Omega) = \int_{\partial\Omega} \mathrm{d}s \leq M$. Thanks to the boundedness of the boundary length and the Lipschitz regularity (see [30] Theorem 2.4.7 p.53 and pp. 50-53), there exists $\varepsilon > 0$ such that all domains $\Omega \in \mathcal{L}ip$ satisfy the ε-cone property [3, 13]: for all $x \in \partial\Omega$, there exists $\xi_x \in \mathbb{R}^2$ with $\|\xi_x\| = 1$ such that for all $y \in \overline{\Omega} \cap B(x, \varepsilon)$

$$C(y, \xi_x, \varepsilon) = \{z \in \mathbb{R}^2 | (z - y, \xi_x) \geq \cos(\varepsilon)\|z - y\| \text{ and } 0 < \|z - y\| < \varepsilon\} \subset \Omega.$$

The constant M can be chosen arbitrary large but finite. We denote by $\Omega_0 \in \mathcal{L}ip$ and $\Gamma_0 \subset \overline{G}$ the "reference" domain and the "reference" boundary respectively (actually $\partial\Omega_0 = \Gamma_D \cup \Gamma_N \cup \Gamma_0$) of the initial shape before optimization.

Thus, the admissible class of domains can be defined as

$$U_{ad}(\Omega_0) = \{\Omega \in \mathcal{L}ip \,|\, \Gamma_D \cup \Gamma_N \subset \partial\Omega,\ \Gamma \subset \overline{G}, \int_\Omega \mathrm{d}x = \mathrm{Vol}(\Omega_0)\}. \tag{14}$$

Hence, in what follows, our purpose is to minimize the acoustic energy in Ω over all admissible shapes Γ, keeping constant the volume of the initial domain Ω_0, *i.e.*, we want to minimize

$$J(\Omega, u) = A\int_\Omega |u|^2 \mathrm{d}x + B\int_\Omega |\nabla u|^2 \mathrm{d}x + C\int_\Gamma |u|^2 d\sigma \tag{15}$$

for the domain $\Omega \in U_{ad}(\Omega_0)$ with $\mathrm{Vol}(\Omega_0) = \int_{\Omega_0} \mathrm{d}x$, $A \geq 0$, $B \geq 0$, $C \geq 0$ positive constants for any fixed $\omega > 0$. In order to keep the volume constraint, instead of Eq. (15) we can also consider the objective function

$$J_1(\Omega, u) = A\int_\Omega |u|^2 \mathrm{d}x + B\int_\Omega |\nabla u|^2 \mathrm{d}x + C\int_\Gamma |u|^2 d\sigma + \mu(\mathrm{Vol}(\Omega) - \mathrm{Vol}(\Omega_0))^2, \tag{16}$$

where μ is some (large) positive constant penalizing the volume variation.

Let us prove the existence of an optimal shape:

Theorem 2. *Let $\Omega_0 \subset D$ be a domain of the class $\mathcal{L}ip$ with a Lipschitz boundary $\partial\Omega_0$ of bounded length, such that $\Gamma_D \cup \Gamma_N \subset \partial\Omega_0$ and $\Gamma_0 = \partial\Omega_0 \setminus (\Gamma_D \cup \Gamma_N) \subset \overline{G}$, U_{ad} be defined by (14) and $\omega > 0$ be fixed. For the objective function $J(\Omega)$, defined in (15), the shape optimization problem $\inf_{\Omega \in U_{ad}(\Omega_0)} J(\Omega)$ has at least one minimum solution (there exists at least one optimal shape Γ).*

Proof. Let us start by noticing that, since all $\Omega \in U_{ad}(\Omega_0)$ are included in the same domain D, it follows that the Poincaré constants in Theorem 1 can all be bounded by the same constant $C(\mathrm{Vol}(D))$ depending only on the volume of D.

Secondly, (see [30] Theorem 2.4.10 p. 56 and p. 145) $U_{ad}(\Omega_0)$ is closed with respect to the Hausdorff convergence (*i.e.* if $(\Omega_n)_{n\in\mathbb{N}^*} \subset U_{ad}(\Omega_0)$ and $d_H(D\setminus\Omega_n, D\setminus\Omega) \to 0$ for $n \to +\infty$, which means that $\Omega_n \to \Omega$ in the sense of Hausdorff, then $\Omega \in U_{ad}(\Omega_0)$), but also in the sense of characteristic functions, (*i.e.* if $(\Omega_n)_{n\in\mathbb{N}^*} \subset U_{ad}(\Omega_0)$ and $\mathbb{1}_{\Omega_n} \to \mathbb{1}_\Omega$ for $n \to +\infty$ in $L^p_{loc}(\mathbb{R}^2)$ for all $p \in [1, \infty[$, then $\Omega \in U_{ad}(\Omega_0)$) and also in sense of compacts (if for all K compact in Ω it follows that $K \subset \Omega_n$ and for all O compact in $D \setminus \overline{\Omega}$ it follows that $O \in D \setminus \overline{\Omega}_n$ for a sufficiently large n, then $\Omega \in U_{ad}(\Omega_0)$).

Let $(\Omega_n)_{n\in\mathbb{N}^*} \subset U_{ad}(\Omega_0)$ be a minimizing sequence of the functional $J(\Omega)$ (it exists since $J(\Omega) \geq 0$). Hence, also by [30] Theorem 2.4.10 p.56, there exist a domain $\Omega \in U_{ad}(\Omega_0)$ and a subsequence $(\Omega_{n_k})_{k\in\mathbb{N}}$ converging in these three senses to Ω and such that $\overline{\Omega}_{n_k}$ and Γ_{n_k} converge in the sense of Hausdorff to $\overline{\Omega}$ and Γ respectively (all other boundary parts are the same as the sequence is in $U_{ad}(\Omega_0)$). In the aim to abbreviate the notations, in what follows the index n_k is changed to n.

Let us consider now the solutions $(u_n)_{n\in\mathbb{N}^*}$ of the Helmholtz problem on $(\Omega_n)_{n\in\mathbb{N}^*}$. Using [13] that the norm of the extension operator $E : H^1(\Omega) \to H^1(\mathbb{R}^2)$ for all $\Omega \in U_{ad}(\Omega_0)$, as domains with Lipschitz boundaries and of finite perimeter, is uniformly bounded, *i.e* there exists a constant $C_E > 0$ independent of n such that

$$\|Eu_n|_D\|_{H^1(D)} \leq C_E \|u_n\|_{H^1(\Omega_n)}, \tag{17}$$

we deduce that the sequence $(Eu_n|_D)_{n\in\mathbb{N}^*}$ is bounded in $H^1(D)$:

$$\begin{aligned}
\|Eu_n|_D\|_{H^1(D)} &\leq C_E \|u_n\|_{H^1(\Omega_n)} \\
&\leq C_E C(\alpha, \omega, C_p(\Omega_n)) \left(\|f\|_{L_2(\Omega_n)} + \|g\|_{H^{\frac{1}{2}}(\Gamma_D)} + \|h\|_{V(\Omega_n)} \right) \\
&\leq C_E C(\alpha, \omega, \mathrm{Vol}(D)) \left(\|f\|_{L_2(D)} + \|g\|_{H^{\frac{1}{2}}(\Gamma_D)} + C_E\|h\|_{V(D)} \right),
\end{aligned}$$

which means that there exists a constant $C > 0$ independent of n such that

$$\|Eu_n|_D\|_{H^1(D)} \leq C \text{ for all } n.$$

Here, in addition to the uniform boundedness of the extension operators, we have also used (10) and the fact that Γ_D is the same for all n. Consequently, there exists $u^* \in H^1(D)$ such that $Eu_n|_D \rightharpoonup u^*$ in $H^1(D)$. By compactness of the trace operator $\mathrm{Tr}_\Gamma : H^1(D) \to L_2(\Gamma)$ and of the inclusion of $H^1(D)$ in $L_2(D)$ (see Theorem 4), we directly have that $\mathrm{Tr}_\Gamma(Eu_n|_D) \to \mathrm{Tr}_\Gamma(u^*)$ in $L_2(\Gamma)$ and $Eu_n|_D \to u^*$ in $L_2(D)$.

Let us show that u^* is equal to the weak solution u of (9) on Ω.

From the variational formulation (9), taking $f \in L_2(D)$ and $h \in V(D)$, let us consider linear functionals defined for a fixed $v \in V(D)$ and for all w_n and w in $V(D)$

$$\begin{aligned} F^n[w_n, v] =& (\nabla w_n, \nabla v)_{L_2(\Omega_n)} - \omega^2 (w_n, v)_{L_2(\Omega_n)} + (\alpha w_n, v)_{L_2(\Gamma_n)} \\ &+ (f, v)_{L_2(\Omega_n)} - (\mathrm{Tr}_{\Gamma_n} h, v)_{L_2(\Gamma_n)}, \\ F[w, v] =& (\nabla w, \nabla v)_{L_2(\Omega)} - \omega^2 (w, v)_{L_2(\Omega)} + (\alpha w, v)_{L_2(\Gamma)} \\ &+ (f, v)_{L_2(\Omega)} - (\mathrm{Tr}_\Gamma h, v)_{L_2(\Gamma)}. \end{aligned}$$

We start by showing that as soon as $w_n \rightharpoonup w$ in $V(D)$

$$\forall v \in V(D) \quad F^n[w_n, v] \to F[w, v] \text{ for } n \to +\infty. \tag{18}$$

Thus we consider

$$\begin{aligned} |F^n[w_n, v] - F[w, v]| \leq & |(\nabla w_n, \mathbb{1}_{\Omega_n} \nabla v)_{L_2(D)} - (\nabla w, \mathbb{1}_\Omega \nabla v)_{L_2(D)}| \\ &+ \omega^2 |(w_n, \mathbb{1}_{\Omega_n} v)_{L_2(D)} - (w, \mathbb{1}_\Omega v)_{L_2(D)}| \\ &+ \left|(\alpha w_n, v)_{L_2(\Gamma_n)} - (\alpha w, v)_{L_2(\Gamma)}\right| + |(f, (\mathbb{1}_{\Omega_n} - \mathbb{1}_\Omega) v)_{L_2(D)}| \\ &+ |(\mathrm{Tr}_{\Gamma_n} h, v)_{L_2(\Gamma_n)} - (\mathrm{Tr}_\Gamma h, v)_{L_2(\Gamma)}|. \end{aligned}$$

Since $\Omega_n \to \Omega$ in the sense of characteristic functions and $v \in H^1(D)$, we directly have that $\mathbb{1}_{\Omega_n} \nabla v \to \mathbb{1}_\Omega \nabla v$ in $L_2(D)$, which with $w_n \rightharpoonup w$ in $V(D)$ gives that

$$(\nabla w_n, \mathbb{1}_{\Omega_n} \nabla v)_{L_2(D)} \to (\nabla w, \mathbb{1}_\Omega \nabla v)_{L_2(D)} \text{ for } n \to +\infty.$$

By the compactness of the inclusion of $H^1(D)$ in $L_2(D)$, $w_n \to w$ in $L_2(D)$ and by the convergence of the characteristic functions $\mathbb{1}_{\Omega_n} v \to \mathbb{1}_\Omega v$ in $L_2(D)$, hence we also have

$$(w_n, \mathbb{1}_{\Omega_n} v)_{L_2(D)} \to (w, \mathbb{1}_\Omega v)_{L_2(D)}$$

and similarly, $(f, (\mathbb{1}_{\Omega_n} - \mathbb{1}_\Omega) v)_{L_2(D)} \to 0$.

Let us prove that

$$\forall v \in C(\overline{D}) \cap V(D) \quad (\alpha w_n, v)_{L_2(\Gamma_n)} \to (\alpha w, v)_{L_2(\Gamma)}. \tag{19}$$

Thanks to [37] Theorem 1.1.6/2, for all domains $\Omega \in U_{ad}(\Omega_0)$ and D itself, the space $C^\infty(\overline{\Omega}) \cap V(\Omega)$ is dense in $V(\Omega)$. Thus there exists a sequence $(\phi_m)_{m \in \mathbb{N}} \subset C^\infty(\overline{D}) \cap V(D)$ converging strongly to $w \in V(D)$. Therefore, following [11] we have

$$\begin{aligned} &\left| \int_{\Gamma_n} \mathrm{Tr} w_n \mathrm{Tr} v \mathrm{d}s - \int_\Gamma \mathrm{Tr} w \mathrm{Tr} v \mathrm{d}s \right| \leq \\ &\leq \left| \int_{\Gamma_n} |\mathrm{Tr} w_n - \mathrm{Tr} w| |\mathrm{Tr} v| \mathrm{d}s \right| + \left| \int_{\Gamma_n} |\mathrm{Tr} w - \mathrm{Tr} \phi_m| |\mathrm{Tr} v| \mathrm{d}s \right| \\ &+ \left| \int_{\Gamma_n} \mathrm{Tr} \phi_m \mathrm{Tr} v \mathrm{d}s - \int_\Gamma \mathrm{Tr} \phi_m \mathrm{Tr} v \mathrm{d}s \right| + \left| \int_\Gamma |\mathrm{Tr} \phi_m - \mathrm{Tr} w| |\mathrm{Tr} v| \mathrm{d}s \right|. \end{aligned} \tag{20}$$

We start by estimating the first term in (20):

$$\left|\int_{\Gamma_n} |\mathrm{Tr} w_n - \mathrm{Tr} w||\mathrm{Tr} v|\mathrm{d}s\right| \leq \|\mathrm{Tr}(w_n - w)\|_{L_2(\Gamma_n)}\|\mathrm{Tr} v\|_{L_2(\Gamma_n)}.$$

Moreover, there exists a positive constant $C_\sigma > 0$ independent of n such that for $\frac{1}{2} < \sigma \leq 1$ it holds

$$\forall w \in H^\sigma(\mathbb{R}^2) \quad \|\mathrm{Tr}_{\Gamma_n} w\|^2_{L_2(\Gamma_n)} \leq C_\sigma \|w\|^2_{H^\sigma(\mathbb{R}^2)}. \tag{21}$$

It is a direct corollary of the proof of [11] Theorem 5.3 and the fact that the lengths of Γ and all Γ_n are finite and bounded by a constant, denoted by M. In addition,

$$\|\mathrm{Tr} v\|_{L_2(\Gamma_n)} \leq \mathrm{Vol}(\Gamma_n)\|v\|_{L^\infty(D)} \leq M\|v\|_{L^\infty(D)}.$$

Moreover, by Theorem 5.8 [11], for D (but also for all domains in $U_{ad}(\Omega_0)$) there exists a bounded linear extension operator $E_\sigma : H^\sigma(D) \to H^\sigma(\mathbb{R}^2)$, $\frac{1}{2} < \sigma \leq 1$, with

$$\|E_\sigma v\|_{H^\sigma(\mathbb{R}^2)} \leq C_D \|v\|_{H^\sigma(D)}. \tag{22}$$

Hence, applying (21) and (22), we obtain that

$$\|\mathrm{Tr}(w_n - w)\|_{L_2(\Gamma_n)} \leq C_\sigma \|E_\sigma(w_n - w)\|_{H^\sigma(\mathbb{R}^2)} \leq C_\sigma C_D \|w_n - w\|_{H^\sigma(D)},$$

from where, by the compactness of the embedding of $H^1(D)$ in $H^\sigma(D)$ for $\frac{1}{2} < \sigma < 1$, we finally have that $\|w_n - w\|_{H^\sigma(D)} \to 0$ for $n \to +\infty$ and consequently the first term in (20) converges to 0 for $n \to +\infty$.

For the second term (and in the same way the last term) in (20), as previously we directly find

$$\left|\int_{\Gamma_n} |\mathrm{Tr} w - \mathrm{Tr}\phi_m||\mathrm{Tr} v|\mathrm{d}s\right| \leq C\|w - \phi_m\|_{H^1(D)} \to 0 \text{ for } m \to +\infty$$

with a constant $C > 0$ independent of n. For the last term we simply replace Γ_n by Γ, knowing that $\Omega \in U_{ad}(\Omega_0)$. Hence, for all $\varepsilon > 0$ there exists $k \in \mathbb{N}$ (uniformly on n) such that

$$\forall m \geq k \quad \max\left\{\left|\int_{\Gamma_n} |\mathrm{Tr} w - \mathrm{Tr}\phi_m||\mathrm{Tr} v|\mathrm{d}s\right|, \left|\int_{\Gamma} |\mathrm{Tr}\phi_m - \mathrm{Tr} w||\mathrm{Tr} v|\mathrm{d}s\right|\right\} < \varepsilon.$$

Thus, let us fix such an m.

Finally, for the third term in (20), it is sufficient to prove that $\int_{\Gamma_n} \mathrm{d}x \to \int_\Gamma \mathrm{d}x$ for $n \to +\infty$, which, by the continuity and the boundedness of $\phi_m v$ in $\overline{D}$ with a standard density argument, implies

$$\int_{\Gamma_n} |\mathrm{Tr}\phi_m \mathrm{Tr} v|\mathrm{d}s \to \int_\Gamma |\mathrm{Tr}\phi_m \mathrm{Tr} v|\mathrm{d}s \text{ for } n \to +\infty. \tag{23}$$

Let us now prove that $\int_{\Gamma_n} \mathrm{d}x \to \int_\Gamma \mathrm{d}x$ for $n \to +\infty$: for a function $g \in H^2(D)$, since D and all Ω_n and Ω are Lipschitz domains in $\mathbb{R}^2$, we have $g \in C(\overline{\Omega}_n)$ and its normal derivative on Γ_n belongs to $L_2(\Gamma_n)$ for all n. We apply the Green formula to integrate by parts

$$\begin{aligned}\left|\int_{\Gamma_n} \frac{\partial g}{\partial \nu} ds - \int_\Gamma \frac{\partial g}{\partial \nu} ds\right| &= \left|\int_{\Omega_n} \Delta g - \int_\Omega \Delta g\right| \\ &= \left|\int_{\mathbb{R}^2} (1_{\Omega_n} - 1_\Omega)\Delta g\right| \leq \|(1_{\Omega_n} - 1_\Omega)\|_{L_2}\|\Delta g\|_{L_2} \to 0,\end{aligned}$$

where, in order to avoid repetitive notations, we have denoted by ν the unit external normal vector to a boundary, and where, in the Green formula, we have used the fact that Ω and Ω_n have the same boundary, except for Γ and Γ_n.

Consequently, for a given $\psi \in H^1(\mathbb{R}^2) \cap C(\mathbb{R}^2)$, there exists a function $g \in H^2(D)$ such that $\frac{\partial g}{\partial \nu} = \mathrm{Tr}\psi$, and, applying the above argument, we get

$$\left| \int_{\Gamma_j} \mathrm{Tr}\psi ds - \int_{\Gamma} \mathrm{Tr}\psi ds \right| \to 0.$$

Therefore, for the sufficiently large m that we have fixed, we also have that

$$\forall \varepsilon > 0 \; \exists p \in \mathbb{N} : \; \forall n \geq p \; \left| \int_{\Gamma_n} |\mathrm{Tr}\phi_m \mathrm{Tr} v| \mathrm{d}s - \int_{\Gamma} |\mathrm{Tr}\phi_m \mathrm{Tr} v| \mathrm{d}s \right| < \varepsilon.$$

Putting all results together for the four terms of (20), we obtain (19), which by the density of $C(\overline{D}) \cap V(D)$ in $V(D)$, also holds for all $v \in V(D)$. Consequently, we also have, as $h \in V(D)$

$$\forall v \in V(D) \quad (\mathrm{Tr}_{\Gamma_n} h, v)_{L_2(\Gamma_n)} \to (\mathrm{Tr}_{\Gamma} h, v)_{L_2(\Gamma)} \quad \text{for } n \to +\infty.$$

This concludes the proof of (18).

Hence, taking $w_n = Eu_n|_D \in V(D)$, *i.e.* the extensions of solutions on Ω_n, which are uniformly bounded and weakly converge to $u^* \in V(D)$, we find that for all $v \in V(D)$

$$0 = F^n[Eu_n|_D, v] \to F[u^*, v] = 0 \text{ for } n \to +\infty.$$

This means that u^* is a weak solution on Ω, and by the uniqueness of the weak solution on Ω, $u^*|_\Omega = u$.

In order to conclude on the existence of a minimum of J, we shall prove that

$$\lim_{n \to +\infty} J(\Omega_n) = J(\Omega),$$

which will be obtained if $(\mathbb{1}_{\Omega_n} Eu_n|_D)_{n \in \mathbb{N}^*}$ converges strongly to $\mathbb{1}_\Omega Eu|_D$ in $V(D)$. Firstly, we find in the same way as previously (see [12]) that

$$\left| \int_{\Gamma_n} |\mathrm{Tr} w_n|^2 \mathrm{d}s - \int_{\Gamma} |\mathrm{Tr} w|^2 \mathrm{d}s \right| \to 0 \quad \text{for } n \to +\infty. \tag{24}$$

Then, once again, by the fact that the weak convergence of $(Eu_n|_D)_{n \in \mathbb{N}^*}$ to $Eu|_D$ in $V(D)$ implies the strong convergence in $L_2(D)$ and by (19) and (24), we find

$$\begin{aligned}
&\lim_{n \to +\infty} \|\mathbb{1}_{\Omega_n} Eu_n|_D\|^2_{V(D)} = \lim_{n \to +\infty} \Big(\omega^2 \|\mathbb{1}_{\Omega_n} Eu_n|_D\|^2_{L_2(D)} - i \int_{\Gamma_n} \mathrm{Im}\,\alpha |\,\mathrm{Tr}\, u_n|^2 \mathrm{d}s \\
&- \int_D \mathbb{1}_{\Omega_n} f \overline{Eu_n|_D} \mathrm{d}x + \int_{\Gamma_n} \mathrm{Tr}\, h \overline{\mathrm{Tr}\, u_n} \mathrm{d}s \Big) = \omega^2 \|\mathbb{1}_\Omega Eu|_D\|^2_{L_2(D)} \\
&- i \int_\Gamma \mathrm{Im}\,\alpha |\,\mathrm{Tr}\, u|^2 \mathrm{d}s - \int_D \mathbb{1}_\Omega f \overline{Eu|_D} \mathrm{d}x + \int_\Gamma \mathrm{Tr}\, h \overline{\mathrm{Tr}\, u} \mathrm{d}s = \|u\|^2_{V(\Omega)}.
\end{aligned}$$

Since we have at the same time the weak convergence and the convergence of norms, it implies the strong convergence in $V(D)$ and hence finishes the proof. □

4 Shape derivative

We respectively denote by Ω_0 and Γ_0 the domain and the boundary of the initial shape before optimization. The optimization step modifies the initial shape of Ω_0 to $\Omega = (Id + \theta)\Omega_0$, according to the map $x \in \Omega_0 \mapsto (x + \theta(x)) \in \Omega$ and following the vector field $\theta \in W^{1,\infty}(\mathbb{R}^2, \mathbb{R}^2)$. Here Id is the identity map $x \in \mathbb{R}^2 \mapsto x \in \mathbb{R}^2$, $W^{1,\infty}(\mathbb{R}^2, \mathbb{R}^2)$ is the space of Lipschitz functions ϕ from $\mathbb{R}^2$ to $\mathbb{R}^2$, such that ϕ and $\nabla\phi$ are uniformly bounded in $\mathbb{R}^2$.

Using the notations $|\cdot|_{\mathbb{R}^2}$ for the Euclidean norm in $\mathbb{R}^2$ and $|\cdot|_{\mathbb{R}^{2\times 2}}$ for the matrices Euclidean norm on $\mathbb{R}^2$, we define the norm on $W^{1,\infty}(\mathbb{R}^2,\mathbb{R}^2)$ by

$$\|\phi\|_{W^{1,\infty}(\mathbb{R}^2,\mathbb{R}^2)} = \sup_{x\in\mathbb{R}^2} \left(|\phi(x)|_{\mathbb{R}^2} + |\nabla\phi(x)|_{\mathbb{R}^{2\times 2}}\right).$$

Hence $\left(W^{1,\infty}(\mathbb{R}^2,\mathbb{R}^2), \|\cdot\|_{W^{1,\infty}(\mathbb{R}^2,\mathbb{R}^2)}\right)$ is a Banach space.

Let us start by introducing the definition of the shape derivative of a function (see [4]). Without loss of generality, we always consider the two dimensional case ($n = 2$).

Definition 1 (Shape derivative)**.** *Let*

$$\mathcal{C}(\Omega_0) = \{\Omega \subset D \,|\, \exists\theta \in W^{1,\infty}(\mathbb{R}^2,\mathbb{R}^2), \|\theta\|_{W^{1,\infty}(\mathbb{R}^2,\mathbb{R}^2)} < 1,\ \Omega = (Id+\theta)\Omega_0\}.$$

The shape derivative of a function $K(\Omega) : \mathcal{C}(\Omega_0) \to \mathbb{R}$ at Ω_0 is defined as the Fréchet derivative in $W^{1,\infty}(\mathbb{R}^2,\mathbb{R}^2)$ at 0 of the function $\theta \mapsto K\left(Id+\theta\right)(\Omega_0)$, i.e.,

$$K\left(Id+\theta\right)(\Omega_0) = K(\Omega_0) + K'(\Omega_0)(\theta) + o(\theta) \quad \textit{with} \quad \lim_{\theta\to 0} \frac{\|o(\theta)\|_{L^\infty(\mathbb{R}^2)}}{\|\theta\|_{W^{1,\infty}(\mathbb{R}^2,\mathbb{R}^2)}} = 0,$$

where $K'(\Omega_0)$ is a continuous linear form on $W^{1,\infty}(\mathbb{R}^2,\mathbb{R}^2)$.

We prove the following theorem:

Theorem 3. *Let Ω_0 be a bounded domain in $\mathbb{R}^2$ with a connected boundary $\partial\Omega_0 \in C^3$, divided in three disjoint parts $\partial\Omega_0 = \Gamma_0 \sqcup \Gamma_D \sqcup \Gamma_N$. Let $\Omega \in U_{ad}(\Omega_0)$, defined in (14), and such that $\partial\Omega = \Gamma \sqcup \Gamma_D \sqcup \Gamma_N$ with $\Gamma = (Id+\theta)\Gamma_0$ ($\theta \in W^{1,\infty}(\mathbb{R}^2,\mathbb{R}^2) \cap C^1(\mathbb{R}^2,\mathbb{R}^2)$ and $\|\theta\|_{W^{1,\infty}} < 1$). Let $u(\Omega_0) \in H^3(\Omega_0)$ be the solution of problem (2) in Ω_0 with $h = 0$, $g \in H^{\frac{5}{2}}(\Gamma_D)$ and $f \in H^1(\mathbb{R}^2)$ (see Theorem 1). Then the shape derivative of the objective function J_1 defined by Eq. (16), is given by*

$$J_1'(\Omega_0)(\theta) = \int_{\Gamma_0} (\theta\cdot n)(-\mathcal{V})\mathrm{d}s, \tag{25}$$

where n is the exterior normal vector on Γ_0, and the velocity $-\mathcal{V}$ is given by

$$\begin{aligned} -\mathcal{V} = \big(A|u|^2 + B|\nabla u|^2 + 2B|\alpha|^2|u|^2 - 4C\mathrm{Re}(\alpha)|u|^2 + CH|u|^2\big) \\ + \mathrm{Re}\left(-\nabla u\cdot\nabla w + \omega^2 uw - fw - \alpha H uw + 2\alpha^2 uw\right) \\ + 2\mu\left(\mathrm{Vol}(\Omega) - \mathrm{Vol}(\Omega_0)\right) \end{aligned} \tag{26}$$

in which H is the curvature of the boundary Γ_0, and $w \in V(\Omega_0)$ ($V(\Omega_0)$ is defined Eq. (8)) is the unique solution of the adjoint problem corresponding to u:

$$\begin{cases} \triangle w + \omega^2 w = -2\left(A\bar{u}(\Omega_0) - B\triangle\bar{u}(\Omega_0)\right) & x\in\Omega_0, \\ w = 0 \quad \textit{on } \Gamma_D, \quad \dfrac{\partial w}{\partial n} = 0 \quad \textit{on } \Gamma_N, \\ \dfrac{\partial w}{\partial n} + \alpha w = -2B\bar{\alpha}\bar{u}(\Omega_0) + 2C\bar{u}(\Omega_0) \quad \textit{on } \Gamma_0. \end{cases} \tag{27}$$

The proof of Theorem 3 uses the notion of Eulerian derivative and Remark 6.29 p. 138 of Ref. [4]. It closely follows the proof of Theorem 6.38 pp. 145–146 of G. Allaire [4] (see also on p. 144 the proof of Corollary 6.36), and hence is omitted.

5 Shape optimization algorithm

We want to solve numerically, using the gradient descent method, the following minimization problem: for $\omega > 0$ and Ω_0 given, find $\Omega^{\mathrm{opt}} \in U_{ad}(\lambda,\Omega_0)$, such that

$$J_1(\Omega^{\mathrm{opt}}) = \min_{\Omega\in U_{ad}(\lambda,\Omega_0)} J_1(\Omega).$$

We notice that if the velocity $\mathcal{V}$, defined in Eq. (26), follows the outward normal direction, or equivalently, if $\theta \cdot n = \mathcal{V}$, then Eq. (25) implies that

$$J_1'(\Omega_0)(\theta) = -\int_{\Gamma_0} \mathcal{V}^2 \mathrm{d}s < 0,$$

which ensures the decreasing behavior of the objective function. In order to calculate the velocity $\mathcal{V}$, we need to know u, the solution of the Helmholtz equation in Ω_0, but also w, the solution of the adjoint problem and the curvature H. Inspired by [4, 42, 43], we construct a shape optimization algorithm composed of the following steps:

(i) Solving the Helmholtz equation (2) and its adjoint problem (27) by a cell-centered finite difference scheme on a square Cartesian mesh covering Ω.

(ii) Calculating the velocity $\mathcal{V}$ of the Robin boundary Γ, based on formula (26), and then extending this velocity in the direction of the normal vector on the whole domain D, or at least around the Robin boundary.

(iii) Solving the level set equation to obtain a new shape.

If $J_1'(\Omega)(\theta) \geq 0$, then Ω is an optimal domain, and the algorithm stops. In order to describe the shape of the domain, we use a concept of level sets. More precisely, the level set function ψ of the domain $\Omega \subset D$ is defined by

$$\begin{cases} \psi(x) = 0 & \text{iff} \quad x \in (\partial\Omega \cap D), \\ \psi(x) < 0 & \text{iff} \quad x \in \Omega, \\ \psi(x) > 0 & \text{iff} \quad x \in (D \setminus \Omega). \end{cases}$$

The level set method, initially devised by S. Osher and J-A. Sethian in Ref. [42], allows, not only to define implicitly the domain, but also to follow easily the propagation of the boundary during the evolution process. Let us take into account a particle $x(t)$ on the boundary, which propagates in time, hence it has the zero-level set all time, *i.e.*, $\psi(x(t), t) = 0$. By the chain rule, it yields that

$$\psi_t + x'(t) \cdot \nabla\psi\left(x(t), t\right) = 0. \tag{28}$$

If $\mathcal{V}$ is the velocity in the outward normal direction of the boundary, *i.e.* $x'(t) \cdot n = \mathcal{V}$, with $n = \frac{\nabla\psi}{|\nabla\psi|}$, then from Eq. (28), we obtain a so-called level set equation

$$\psi_t + \mathcal{V}|\nabla\psi| = 0, \tag{29}$$

associated with the initial condition $\psi|_{t=0} = \psi_0(x)$, defined by the signed distance function

$$\psi_0(x) = \pm \mathrm{dist}[x, \Gamma], \quad x \in D. \tag{30}$$

In the last formula, Γ is the Robin boundary, and the sign plus (or minus) corresponds to outside (or inside) of the domain Ω. This equation is of Hamilton-Jacobi type, and in what follows we call it the Hamilton-Jacobi equation. Let us notice, that we need to calculate the solution of the Hamilton-Jacobi equation (29) not only in Ω, but in D, and thus, we need to know $\mathcal{V}$ for all $x \in D$. Hence, knowing initially $\mathcal{V}$ only in Ω by formula (26), we need to extend it to all D. More precisely, to calculate numerically $-\mathcal{V}$ on Ω (see Eq. (26)), we first find numerically the solutions u of the Helmholtz problem (2) and w of the adjoint problem (27) and then evaluate ∇u and ∇w. The curvature H is calculated, on the basis of the level set function ψ, by the following equality

$$H = \nabla \cdot \frac{\nabla\psi}{|\nabla\psi|} = \frac{\psi_{yy}\psi_x^2 - 2\psi_x\psi_y\psi_{xy} + \psi_{xx}\psi_y^2}{\left(\psi_x^2 + \psi_y^2\right)^{3/2}}.$$

Once we know $\mathcal{V}$ in Ω, we extend it outside of the domain [41, 43], solving until the stationary state the equation

$$\phi_t + \beta(x,y)\nabla\phi \cdot n = 0,$$

with the initial condition $\phi(t=0)$ equal to $\mathcal{V}$ inside the domain Ω and zero elsewhere. Here n is defined everywhere in D by $\frac{\nabla\psi}{|\nabla\psi|}$ and β is zero or one corresponding to inside or outside of the domain Ω.

In the aim to penalize too complicated geometries of Γ, the mesh, used to solve the Hamilton-Jacobi equation, is chosen coarser than the mesh used to solve the Helmholtz equation. We use an upwind scheme for solving the Hamilton-Jacobi equation [41, 43] and discretize Eq. (29) as follows

$$\frac{\psi_{ij}^{n+1} - \psi_{ij}^{n}}{\Delta t} + \left[\max\left(V_{ij},0\right)\nabla^{+} + \min\left(V_{ij},0\right)\nabla^{-}\right] = 0, \tag{31}$$

where

$$\begin{aligned}
\nabla^{+} &= \left[\max\left(D_{ij}^{-x},0\right)^2 + \min\left(D_{ij}^{+x},0\right)^2 + \max\left(D_{ij}^{-y},0\right)^2 + \min\left(D_{ij}^{+y},0\right)^2\right]^{1/2},\\
\nabla^{-} &= \left[\max\left(D_{ij}^{+x},0\right)^2 + \min\left(D_{ij}^{-x},0\right)^2 + \max\left(D_{ij}^{+y},0\right)^2 + \min\left(D_{ij}^{-y},0\right)^2\right]^{1/2},\\
D_{ij}^{-x} &= \frac{\psi^n(i,j) - \psi^n(i-1,j)}{\Delta x}, \quad D_{ij}^{+x} = \frac{\psi^n(i+1,j) - \psi^n(i,j)}{\Delta x},\\
D_{ij}^{-y} &= \frac{\psi^n(i,j) - \psi^n(i,j-1)}{\Delta y}, \quad D_{ij}^{+y} = \frac{\psi^n(i,j+1) - \psi^n(i,j)}{\Delta y},
\end{aligned}$$

and $\psi|_{t=0} = \psi_0$ is the signed distance function, defined in (30). With a space-step $\Delta x = \Delta y$ scheme (31) is stable under the following CFL condition

$$\Delta t \leq \frac{\Delta x}{\max(|\mathcal{V}(x,y)|)\sqrt{2}}. \tag{32}$$

6 Numerical experiments

For all numerical tests, presented below, we consider the rectangle $\overline{D} = [0,3]\times[0,1]$, and suppose that D always contains the domain Ω, on which we solve the Helmholtz equation. The boundaries Γ_N and Γ_D are fixed, as it is shown on Figure 1, and Γ is the moving boundary inside of $\overline{G} = [\frac{3}{2},3]\times[0,1]$. The initial $\Omega_0 =]0,2[\times]0,1[$ has a flat boundary Γ_0 fixed at $x=2$. The characteristic lengths of Ω_0 are $\ell = 1$ and $L = 2\ell$.

The Helmholtz equation is considered with a wave number $k = \frac{\omega}{c_0}$, *i.e*,

$$\Delta u + k^2 u = -f,$$

where c_0 is the sound speed in air. We take

$$f = 0, \quad g = \frac{1}{\sigma\sqrt{2\pi}}\exp\left(-\frac{(y-1/2)^2}{2\sigma^2}\right)$$

with $\sigma = 1$ in the Helmholtz boundary value problem. For the chosen σ, the smallest wavelength, excited by g, is $\lambda = \frac{\ell}{2}$. The parameter α in the Robin boundary condition depends on the value of the frequency ω. It is calculated for ISOREL, using a minimization of the difference between the solution of the problem with a volume dissipation (described by a damped wave equation) and the solution of the problem with the boundary dissipation for the flat shape of Γ (see Theorem 5). We solve the Helmholtz boundary value problem on a fine mesh with the size $h = \frac{\ell}{64}$. For waves with the wavelength equal to $\frac{\ell}{2}$, this typically gives dispersion errors of the order 10^{-3}, since the dispersion error due to the centered finite difference approximation of the Laplacian is known to be $\frac{(kh)^2}{24}$, with $kh = \frac{2\pi}{32}$ here. We perform the level set approach for the optimization algorithm on the coarse mesh of the size $\kappa = 2h = \frac{\ell}{32}$ (in the aim of a penalization of too much complicated shapes of Γ). However, we notice that $\kappa \ll \lambda$.

6.1 Properties of the optimization algorithm

Let us illustrate the stability properties of the optimization algorithm.

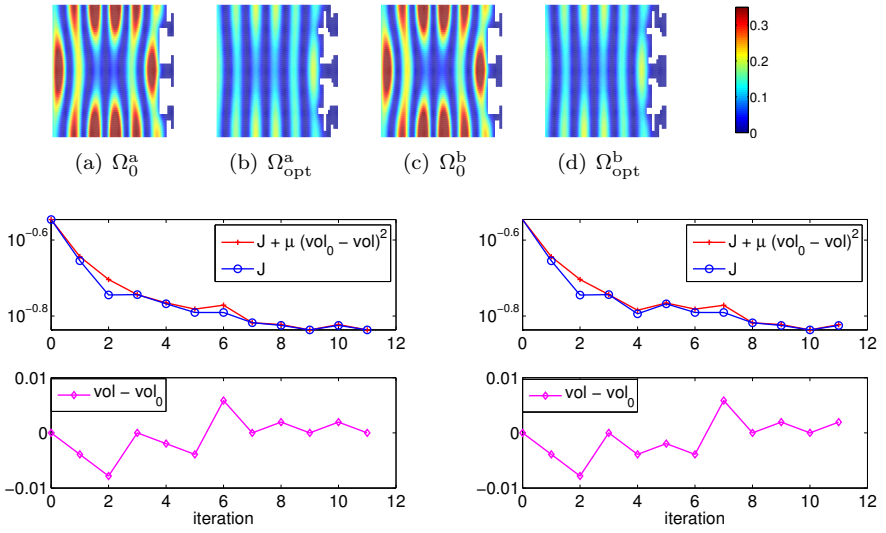

(a) Ω_0^a (b) Ω_{opt}^a (c) Ω_0^b (d) Ω_{opt}^b

(f) Convergence starting by Ω_0^a (g) Convergence starting by Ω_0^b

Figure 2: The values of $|u|^2$ are presented on two initial and optimal domains for the fixed frequency $\omega_0 = 3170$. From left to right: the initial domain Ω_0^a and the corresponding optimal domain $\Omega_{\text{opt}}^a = \Omega_{11}^a$, the initial domain Ω_0^b, taken in a small neighborhood of Ω_0^a, and the corresponding optimal domain $\Omega_{\text{opt}}^b = \Omega_{10}^b$. We see that Ω_{opt}^a is in a small neighborhood of Ω_{opt}^b (the shapes of Γ^a and Γ^b are almost the same). The values of J are also almost the same: $J(\Omega_{\text{opt}}^a)(\omega_0) \approx 0.1458$ and $J(\Omega_{\text{opt}}^b)(\omega_0) \approx 0.1458$. As compared to the flat shape $\overline{\Omega}_0 = [0,2] \times [0,1]$, for which $J(\Omega_0)(\omega_0) = 4.286$, we have $J(\Omega_0)(\omega_0)/J(\Omega_{\text{opt}}^a)(\omega_0) = 27.492$, hence the optimal shapes dissipate the energy 27.5 times better than the flat one. The bottom pictures show the convergence of the optimization algorithm for two cases of initial domain: for Ω_0^a in the left and for Ω_0^b in the right.

We fix the frequency $\omega_0 = 3170$, which is a local maximum of

$$J(\Omega)(\omega) = \int_\Omega |u|^2 \mathrm{d}x,$$

calculated for $\Omega_0 =]0,2[\times]0,1[$ in a range of frequencies, for instance, $\omega \in [3000, 6000]$. This time we chose $A = 1$ and $B = C = 0$ for the simulation of the acoustical energy.

If we start the optimization algorithm one time from $\Omega_0 = \Omega_0^a$ and the second time from $\Omega_0 = \Omega_0^b$, such that the Hausdorff distance $d_H(\Omega_0^a, \Omega_0^b) < \varepsilon$ is small enough, then the optimal shapes Ω_{opt}^a and Ω_{opt}^b are "almost the same", *i.e.* there exists $C > 0$, depending only on ε, such that the Hausdorff distance

$$d_H(\Omega_{\text{opt}}^a, \Omega_{\text{opt}}^b) < C(\varepsilon) d_H(\Omega_0^a, \Omega_0^b)$$

is also small. Hence, $|J(\Omega_{\text{opt}}^a)(\omega_0) - J(\Omega_{\text{opt}}^b)(\omega_0)| \ll 1$ is also small by the continuity of J as a function of the domain; see Figure 2 for a numerical example.

Let us also notice, that, as for the question of Mark Kac "Can one hear the shape of a drum?" [25, 26, 24], we don't have the uniqueness of the optimal shape Γ, since different shapes can have the same spectrum and be identically efficient in the dissipation of the energy in the fixed range of frequency. Figure 3 illustrates the case, when the initial shape

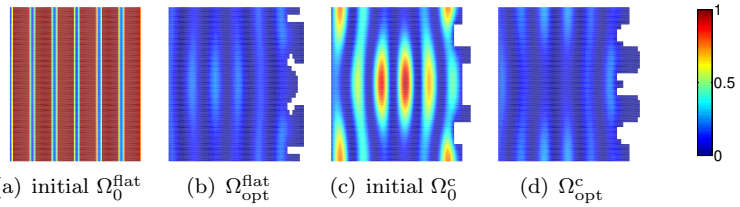

(a) initial Ω_0^{flat} (b) $\Omega_{\text{opt}}^{\text{flat}}$ (c) initial Ω_0^{c} (d) $\Omega_{\text{opt}}^{\text{c}}$

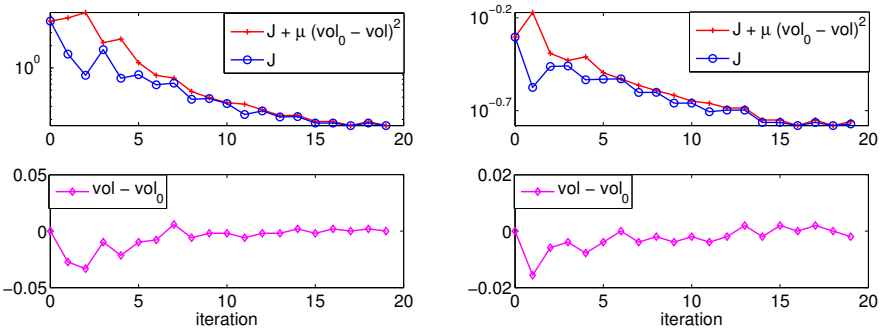

(f) Convergence starting by Ω_0^{flat} (g) Convergence starting by Ω_0^{c}

Figure 3: The values of $|u|^2$ are presented on two initial and optimal domains for the fixed frequency $\omega_0 = 3170$. From left to right: the initial domain Ω_0^{flat} and the corresponding optimal domain $\Omega_{\text{opt}}^{\text{flat}}$, the initial domain Ω_0^{c}, significantly different to Ω_0^{flat} and to $\Omega_{\text{opt}}^{\text{flat}}$, taken with characteristic geometric scales which are almost the same as for $\Omega_{\text{opt}}^{\text{flat}}$, and the corresponding optimal domain Ω_{opt}^{c}. We see that $\Omega_{\text{opt}}^{\text{flat}}$ is not in a small neighborhood of $\Omega_{\text{opt}}^{\text{c}}$ (the shapes of Γ^a and Γ^b are really different). But the values of J for $\omega_0 = 3170$ are also almost the same: $J(\Omega_{\text{opt}}^{\text{flat}}) = 0.1654$ and $J(\Omega_{\text{opt}}^{\text{c}}) = 0.1659$.

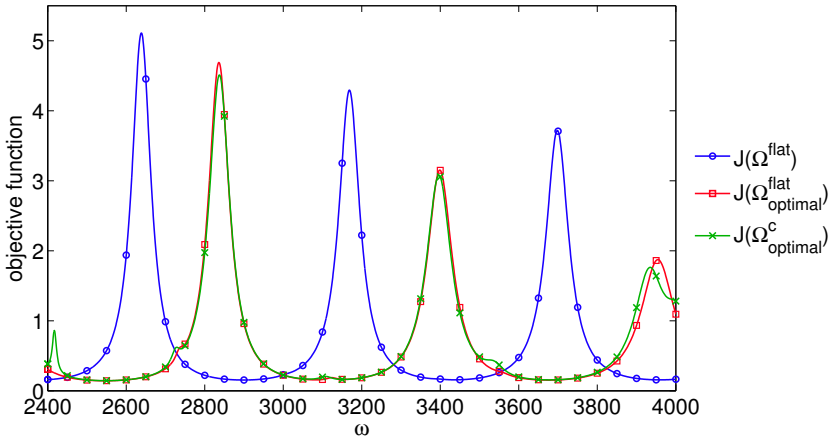

Figure 4: The objective function J as a function of ω for the flat shape Ω_0, for the optimal shape $\Omega_{\text{opt}}^{\text{flat}}$ (see Figure 3) and for the optimal shape Ω_{opt}^{c} (see Figure 3).

$\Omega_0 = \Omega_0^c$ is not in a small neighborhood of Ω_{opt}^a and the characteristic geometric scales of Ω_0^c are almost the same as for Ω_{opt}^a. For this choice of Ω_0^c we obtain that Ω_{opt}^c is not in a small neighborhood of $\Omega_{\text{opt}}^{\text{flat}}$, but we still have $|J(\Omega_{\text{opt}}^c)(\omega_0) - J(\Omega_{\text{opt}}^a)(\omega_0)| \ll 1$. Moreover, Figure 4 shows, that the values of the functional $|J(\Omega_{\text{opt}}^c)(\omega) - J(\Omega_{\text{opt}}^a)(\omega)| \ll 1$ are almost

the same for all ω in a rather large neighborhood of ω_0.

Figure 4 also shows that the minimization process for one given frequency (here $\omega_0 = 3170$, corresponding to the middle peak of $J(\Omega^{\text{flat}})$) is very efficient, but it creates peaks at other frequencies, and so, we need a strategy to find the most efficient shape, able to dissipate the acoustical energy in a large range of frequencies.

6.2 Optimized "simple" wall for a large range of frequencies

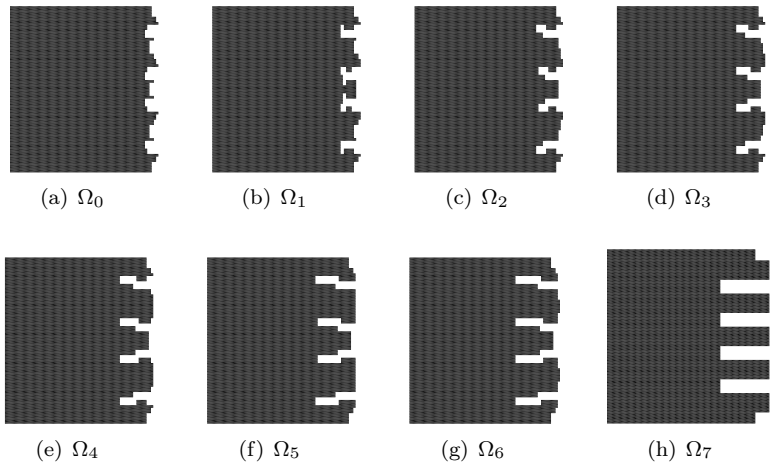

(a) Ω_0 (b) Ω_1 (c) Ω_2 (d) Ω_3

(e) Ω_4 (f) Ω_5 (g) Ω_6 (h) Ω_7

Figure 5: Shapes, which are used in the optimization algorithm process: from left to right in the top line- Ω_0 (the initial shape), Ω_k, $k = 1, 2, 3$, and from left to right in the bottom line - Ω_k, $k = 4, 5, 6, 7$. The domain Ω_7 is generated manually in the aim to simplify the final shape Ω_6.

In this subsection, we are searching a shape of the wall Ω, which could be as absorbing as possible in terms of the acoustic energy $J(\Omega)(\omega) = \int_\Omega |u|^2 \mathrm{d}x$ in a large range of frequencies with the simplest possible design. Let us fix the range of frequencies for the energy dissipation: $\omega \in [3000, 6000]$.

As in subsection 6.1, we fix the frequency $\omega_0 = 3170$ of a local maximum of J on $\Omega_{\text{flat}} =]0, 2[\times]0, 1[$. We perform the shape optimization algorithm for this frequency, taking as the initial shape Ω_0, given on Figure 5, and we obtain Ω_1, optimal at $\omega = 3170$. Noticing that all local maxima of $J(\Omega_1)$ are smaller than the local maxima of $J(\Omega_{\text{flat}})$ (see Figure 6), we choose Ω_1 as the initial domain and restart the optimization algorithm, minimizing in the neighborhood of Ω_1 the sum of functionals $\sum_{k=1}^{3} J(\Omega)(\omega_k)$, where $\omega_1 = 3410$, $\omega_2 = 4025$ and $\omega_3 = 4555$ are the local maxima of $J(\Omega_1)$. This minimization gives the optimal shape Ω_2, such that

1. Ω_2 is almost optimal in the neighborhood of ω_k for $k = 0, 1, 2, 3$;
2. all local maxima of $J(\Omega_2)$ are smaller than the local maxima of $J(\Omega_1)$.

Choosing $\omega_4 = 3625$ and $\omega_5 = 4240$, corresponding to the local maxima of $J(\Omega_2)$, we take Ω_2 as the initial domain and restart the optimization algorithm, minimizing $J(\Omega)(\omega_4)+J(\Omega)(\omega_5)$ to obtain the optimal shape Ω_3, such that

1. Ω_3 is almost optimal in the neighborhood of ω_k for $k = 0, \ldots, 5$;
2. all local maxima of $J(\Omega_3)$ are smaller than the local maxima of $J(\Omega_2)$.

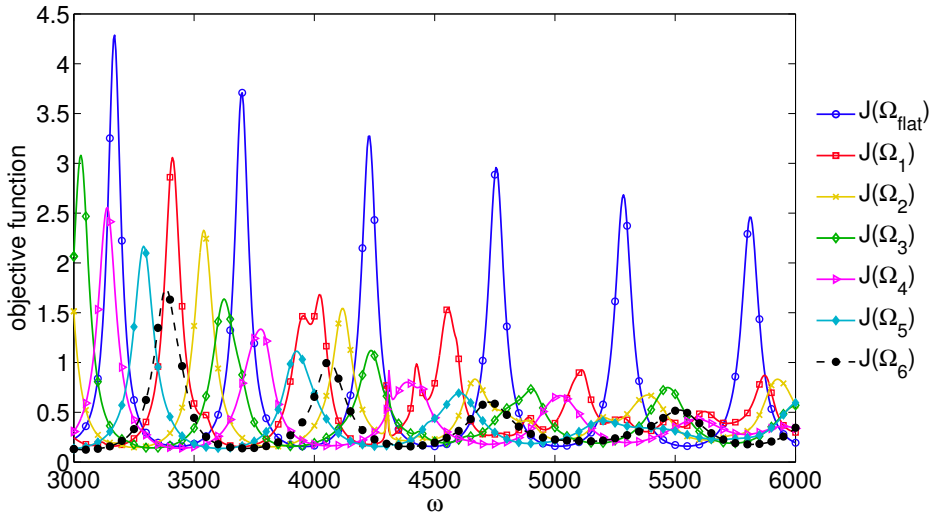

Figure 6: The values of the objective function $J(\Omega_0)$ $(A = 1, B = 0, C = 0)$ for the flat shape as a function of $\omega \in [3000, 6000]$ are presented by the line with circles, the values of $J(\Omega_1)$ (see Figure 5 for the shape of Ω_1) are presented by the line with squares, the values of $J(\Omega_2)$ by the line with stars, those of $J(\Omega_3)$ by the line with empty rhombus, those of $J(\Omega_4)$ by the line with arrows, those of $J(\Omega_5)$ by the line with full rhombus, and those of $J(\Omega_6)$ by the black dash-dotted line.

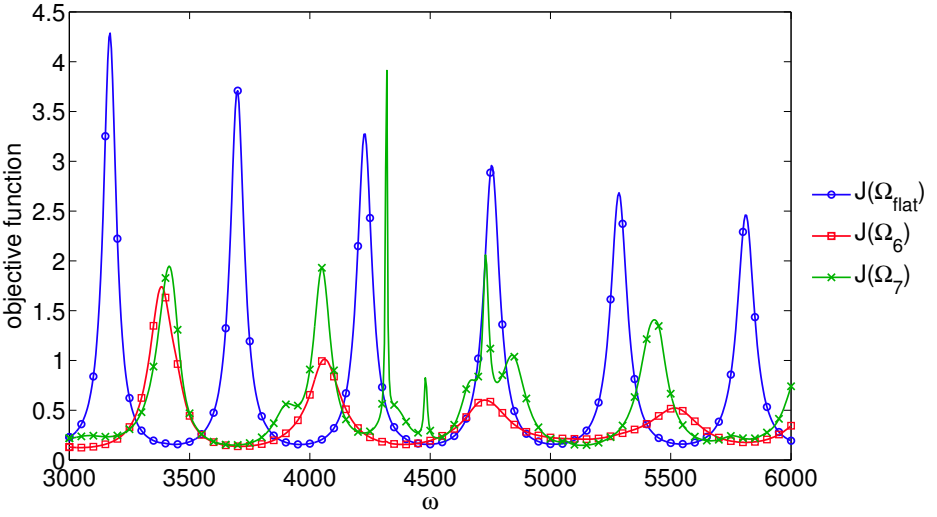

Figure 7: Comparison of the dissipative properties of the flat shape Ω_{flat}, the optimal Ω_6 and of its simplification Ω_7. The values of $J(\Omega_{\text{flat}})$, of $J(\Omega_6)$ and of $J(\Omega_7)$ $(A = 1, B = 0, C = 0)$ as functions of $\omega \in [3000, 6000]$ are given by the lines with circles, squares and stars respectively.

We iterate this process up to Ω_6 and we are stopped by the restriction that Γ must be contained in the area $\overline{G} = [\frac{3}{2}, 3] \times [0, 1]$.

The shape of Ω_6 contains multiscale details, which ensures the dissipative performances of the wall in a large range of frequencies (see Figure 6). Thinking about the demolding

process of wall construction, we simplify the geometry of Ω_6, deleting the multi-scales and keeping only the largest characteristic scale of Ω_6 (see the domain Ω_7, generated by hand, on Figure 5). As we can see from Figure 7, since we have kept almost unchanged the largest characteristic geometric size for Ω_6 and Ω_7, the energy dissipation is also almost the same in the corresponding range of frequencies (see red and green lines for $[3000, 3700]$ on Figure 7). As all smaller scale details have been deleted, the shape of Ω_7 is not as good as the shape of Ω_6 to dissipate higher frequencies (see lines with squares and stars for $[3700, 6000]$ on Figure 7). Hence, Figure 7 shows that the compromises between two desired properties "to be the most dissipative" (as Ω_6 here) and "to be simple to construct" (on the example of Ω_7) is not too bad, especially if we know the most important frequencies to dissipate.

Figures 8–10 show the energy distribution for three values of frequencies illustrating the three typical cases: $J(\Omega_6) \approx J(\Omega_7)$, $J(\Omega_6) < J(\Omega_7)$ and $J(\Omega_7)$ has its local maximum (see Figure 7).

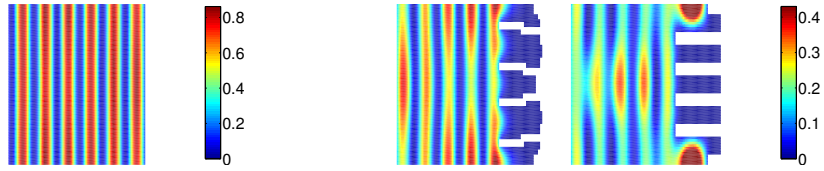

(a) $|u(\Omega_{\text{flat}})|^2$ (c) $|u(\Omega_6)|^2$ (d) $|u(\Omega_7)|^2$

Figure 8: Energy distribution in Ω_{flat}, Ω_6 and Ω_7 respectively for $\omega = 3235$, corresponding to the case when $J(\Omega_6) \approx J(\Omega_7)$ are almost the same (precisely $J(\Omega_6) = 0.2841$, $J(\Omega_7) = 0.2829$)

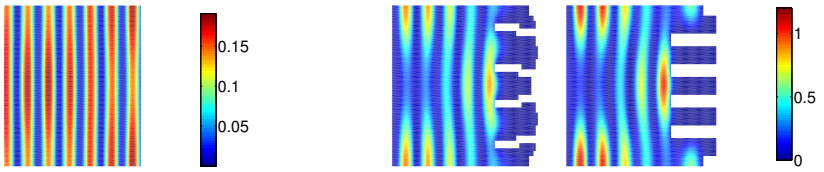

(a) $|u(\Omega_{\text{flat}})|^2$ (c) $|u(\Omega_6)|^2$ (d) $|u(\Omega_7)|^2$

Figure 9: Energy distribution in Ω_{flat}, Ω_6 and Ω_7 respectively for $\omega = 3495$, corresponding to the case when $J(\Omega_6) = 0.4767$ and $J(\Omega_7) = 0.5077$ take slight different values.

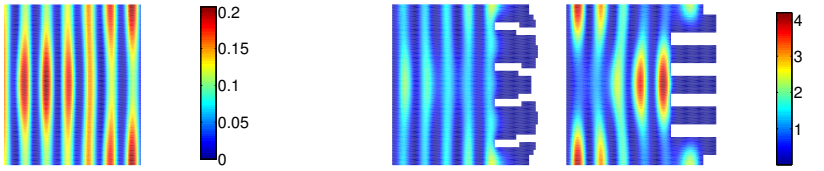

(a) $|u(\Omega_{\text{flat}})|^2$ (c) $|u(\Omega_6)|^2$ (d) $|u(\Omega_7)|^2$

Figure 10: Energy distribution in Ω_{flat}, Ω_6 and Ω_7 respectively for $\omega = 3415$, the frequency which yields a local maximum of the objective function on the domain Ω_7.

7 Conclusion

Started by the well-posedness result on the largest class of domains with d-set boundaries including even fractal boundaries, we showed that the problem of finding an optimal shape for the Helmholtz problem with a dissipative boundary has at least one solution. We developed an algorithm and numerical methods allowing to calculate optimal shapes numerically. With the purpose to find the most efficient and the simplest, easy to construct, shape of a noise absorbing wall to dissipate the energy of a sound wave in a range of frequencies, we show numerically that if we simplify the obtained optimal shape, by deleting the smaller scales of the geometry, the new shape is efficient in the frequencies corresponding to its characteristic geometry scale length, but no more efficient in the higher frequencies.

A d-sets and trace theorems on a d-set

Let us define the main notions which we use in Theorem 1.

Definition 2 (Ahlfors d-regular set or d-set [31]). *Let F be a Borel subset of $\mathbb{R}^n$ and m_d be the d-dimensional Hausdorff measure, $0 < d \leq n$, $d \in \mathbb{R}$. The set F is called a d-set, if there exist positive constants c_1, $c_2 > 0$,*

$$c_1 r^d \leq m_d(F \cap B_r(x)) \leq c_2 r^d, \quad \text{for } \forall\, x \in F,\ 0 < r \leq 1,$$

where $B_r(x) \subset \mathbb{R}^n$ denotes the Euclidean ball centered at x and of radius r.

In particular, n-sets (d-set with $d = n$) satisfy

$$\exists c > 0 \quad \forall x \in \overline{\Omega},\ \forall r \in]0, \delta[\cap]0, 1] \quad m(B_r(x) \cap \Omega) \geq C m(B_r(x)) = c r^n,$$

where $m(A)$ denotes the Lebesgue measure of a set A. This property is also called the measure density condition [28]. Let us notice that an n-set Ω cannot be "thin" close to its boundary $\partial\Omega$.

The trace operator on a d-set is understood in the following way:

Definition 3 (Trace operator). *For an arbitrary open set Ω of $\mathbb{R}^n$, the trace operator* Tr *is defined [31] for $u \in L^1_{loc}(\Omega)$ by*

$$\operatorname{Tr} u(x) = \lim_{r \to 0} \frac{1}{m(\Omega \cap B_r(x))} \int_{\Omega \cap B_r(x)} u(y) \mathrm{d}y,$$

where m denotes the Lebesgue measure. The trace operator Tr *is considered for all $x \in \overline{\Omega}$ for which the limit exists.*

Hence, the following Theorem (see Ref. [6] Section 2) generalizes the classical results [35, 36] for domains with the Lipschitz boundaries $\partial\Omega$:

Theorem 4. *Let Ω be an admissible domain in $\mathbb{R}^n$ in the sense of Ref. [6], i.e. Ω is an n-set, such that its boundary $\partial\Omega$ is a compact d-set, $n - 2 < d < n$, and the norms $\|f\|_{H^1(\Omega)}$ and $\|f\|_{C^1_2(\Omega)} = \|f\|_{L_2(\Omega)} + \|f^\sharp_{1,\Omega}\|_{L_2(\Omega)}$ with*

$$f^\sharp_{1,\Omega}(x) = \sup_{r>0} r^{-1} \inf_{c \in \mathbb{R}} \frac{1}{\mu(B_r(x))} \int_{B_r(x) \cap \Omega} |f(y) - c| \mathrm{d}y$$

are equivalent on $H^1(\Omega)$. Then,

1. *$H^1(\Omega)$ is compactly embedded in $L_2^{loc}(\Omega)$ or in $L_2(\Omega)$ if Ω is bounded;*
2. *$\operatorname{Tr}_\Omega : H^1(\mathbb{R}^n) \to H^1(\Omega)$ is a linear continuous and surjective operator with linear bounded inverse (the extension operator $E_\Omega : H^1(\Omega) \to H^1(\mathbb{R}^n)$);*

3. *for* $\beta = 1-(n-d)/2 > 0$ *the operators* $\mathrm{Tr} : H^1(\mathbb{R}^n) \to L_2(\partial\Omega)$, *and* $\mathrm{Tr}_{\partial\Omega} : H^1(\Omega) \to L_2(\partial\Omega)$ *are linear compact operators with dense image* $\mathrm{Im}(\mathrm{Tr}) = \mathrm{Im}(\mathrm{Tr}_{\partial\Omega}) = B^{2,2}_{\beta}(\partial\Omega)$ *and with linear bounded right inverse (the extension operators)* $E : B^{2,2}_{\beta}(\partial\Omega) \to H^1(\mathbb{R}^n)$ *and* $E_{\partial\Omega} : B^{2,2}_{\beta}(\partial\Omega) \to H^1(\Omega)$;

4. *the Green formula holds for all* u *and* v *from* $H^1(\Omega)$ *with* $\Delta u \in L_2(\Omega)$*:*

$$\int_\Omega v\Delta u\mathrm{d}x + \int_\Omega \nabla v.\nabla u\mathrm{d}x = \langle \frac{\partial u}{\partial \nu}, \mathrm{Tr}v\rangle_{((B^{2,2}_{\beta}(\partial\Omega))',B^{2,2}_{\beta}(\partial\Omega))}, \tag{33}$$

where the dual Besov space $(B^{2,2}_{\beta}(\partial\Omega))' = B^{2,2}_{-\beta}(\partial\Omega)$ *is introduced in Ref. [32].*

5. *the usual integration by parts holds for all* u *and* v *from* $H^1(\Omega)$ *in the following weak sense*

$$\langle u\nu_i, v\rangle_{(B^{2,2}_{\beta}(\partial\Omega))',B^{2,2}_{\beta}(\partial\Omega))} := \int_\Omega \frac{\partial u}{\partial x_i}v\mathrm{d}x + \int_\Omega u\frac{\partial v}{\partial x_i}\mathrm{d}x \quad i = 1,\ldots,n, \tag{34}$$

where by $u\nu_i$ *is denoted the linear continuous functional on* $B^{2,2}_{\beta}(\partial\Omega)$.

6. $\|u\|_{H^1(\Omega)}$ *is equivalent to* $\|u\|_{\mathrm{Tr}} = \left(\int_\Omega |\nabla u|^2\mathrm{d}x + \int_{\partial\Omega} |\mathrm{Tr}u|^2\mathrm{d}m_d\right)^{\frac{1}{2}}$.

Theorem 4 is a particular case of the results proven in Ref. [6]. We also notice that in the framework of the Sobolev space H^1 and the Besov spaces $B^{2,2}_{\beta}$ with $\beta < 1$, as here, we do not need to impose Markov's local inequality on $\partial\Omega$ (see Ref. [31] p.39), as it is trivially satisfied (see Ref. [33] p. 198). To prove formula (34) we follow the proof of formula (4.11) of Theorem 4.5 in [15] using the existence of a sequence of domains $(\Omega_m)_{m\in\mathbb{N}^*}$ with Lipschitz boundaries such that $\Omega_m \subset \Omega_{m+1}$ and $\Omega = \cup_{m=1}^{\infty}\Omega_m$.

B Approximation of the damping parameter α in the Robin boundary condition by a model with dissipation in the volume

Theorem 5. *Let* $\Omega =]-L, L[\times]-\ell, \ell[$ *be a domain with a simply connected sub-domain* Ω_0*, whose boundaries are* $]-L, 0[\times\{\ell\}$*,* $\{-L\} \times]-\ell, \ell[$*,* $]-L, 0[\times\{-\ell\}$ *and another boundary, denoted by* Γ*, which is the straight line starting in* $(0, -\ell)$ *and ending in* $(0, \ell)$*. In addition let* Ω_1 *be the supplementary domain of* Ω_0 *in* Ω*, so that* Γ *is the common boundary of* Ω_0 *and* Ω_1*. The length* L *is supposed to be large enough.*

Let the original problem (the frequency version of the wave damped problem (1)) be

$$-\nabla\cdot(\mu_0\nabla u_0) - \omega^2\xi_0 u_0 = 0 \quad \text{in } \Omega_0, \tag{35}$$

$$-\nabla\cdot(\mu_1\nabla u_1) - \omega^2\tilde{\xi}_1 u_1 = 0 \quad \text{in } \Omega_1, \tag{36}$$

with

$$\tilde{\xi}_1 = \xi_1\left(1 + \frac{ai}{\xi_1\omega}\right),$$

together with boundary conditions on Γ

$$u_0 = u_1 \quad \text{and} \quad \mu_0\nabla u_0\cdot n = \mu_1\nabla u_1\cdot n, \tag{37}$$

and the condition on the left boundary

$$u_0(-L, y) = g(y), \tag{38}$$

and some other boundary conditions. Let the modified problem be

$$-\nabla \cdot (\mu_0 \nabla u_2) - \omega^2 \xi_0 u_2 = 0 \quad in\ \Omega_0 \tag{39}$$

with boundary absorption condition on Γ

$$\mu_0 \nabla u_2 \cdot n + \alpha u_2 = 0 \tag{40}$$

and the condition on the left boundary

$$u_2(-L, y) = g(y). \tag{41}$$

Let u_0, u_1, u_2 *and* g *be decomposed into Fourier modes in the* y *direction, denoting by* k *the associated wave number. Then the complex parameter* α*, minimizing the following expression*

$$A||u_0 - u_2||^2_{L_2(\Omega_0)} + B||\nabla(u_0 - u_2)||^2_{L_2(\Omega_0)}$$

can be found from the minimization of the error function

$$e(\alpha) := \sum_{k=\frac{n\pi}{L}, n\in\mathbb{Z}} e_k(\alpha),$$

where e_k *are given by*

$$\begin{aligned} e_k(\alpha) = (A + B|k|^2) \Bigg(& \frac{1}{2\lambda_0} \left\{ |\chi|^2 \left[1 - \exp(-2\lambda_0 L)\right] \right. \\ & \left. + |\eta|^2 \left[\exp(2\lambda_0 L) - 1\right] \right\} + 2L \mathrm{Re}\left(\chi \bar{\eta}\right) \Bigg) \\ & + B \frac{\lambda_0}{2} \left\{ |\chi|^2 \left[1 - \exp(-2\lambda_0 L)\right] + |\eta|^2 \left[\exp(2\lambda_0 L) - 1\right] \right\} - 2B\lambda_0^2 L \mathrm{Re}\left(\chi \bar{\eta}\right) \end{aligned}$$

if $k^2 \geq \frac{\xi_0}{\mu_0}\omega^2$ *or*

$$\begin{aligned} & e_k(\alpha) = (A + B|k|^2) \left(L(|\chi|^2 + |\eta|^2) + \frac{i}{\lambda_0} \mathrm{Im}\left\{ \chi \bar{\eta} \left[1 - \exp(-2\lambda_0 L)\right] \right\} \right) \\ & + BL|\lambda_0|^2 \left(|\chi|^2 + |\eta|^2 \right) + iB\lambda_0 \mathrm{Im}\left\{ \chi \bar{\eta} \left[1 - \exp(-2\lambda_0 L)\right] \right\} \end{aligned}$$

if $k^2 < \frac{\xi_0}{\mu_0}\omega^2$*, in which*

$$\begin{aligned} f(x) &= (\lambda_0\mu_0 - x)\exp(-\lambda_0 L) + (\lambda_0\mu_0 + x)\exp(\lambda_0 L), \\ \chi(k,\alpha) &= g_k \left(\frac{\lambda_0\mu_0 - \lambda_1\mu_1}{f(\lambda_1\mu_1)} - \frac{\lambda_0\mu_0 - \alpha}{f(\alpha)} \right), \\ \eta(k,\alpha) &= g_k \left(\frac{\lambda_0\mu_0 + \lambda_1\mu_1}{f(\lambda_1\mu_1)} - \frac{\lambda_0\mu_0 + \alpha}{f(\alpha)} \right), \end{aligned}$$

where

$$\begin{cases} \lambda_0 = \sqrt{k^2 - \frac{\xi_0}{\mu_0}\omega^2} & if \quad k^2 \geq \frac{\xi_0}{\mu_0}\omega^2, \\ \lambda_0 = i\sqrt{\frac{\xi_0}{\mu_0}\omega^2 - k^2} & if \quad k^2 \leq \frac{\xi_0}{\mu_0}\omega^2. \end{cases} \tag{42}$$

Proof. First of all,

$$e(\alpha) := A||u_0 - u_2||^2_{L_2(\Omega_0)} + B||\nabla(u_0 - u_2)||^2_{L_2(\Omega_0)}$$

can be decomposed as a sum of $e_k(\alpha)$

$$e(\alpha) := \sum_{k=\frac{n\pi}{L}, n\in\mathbb{Z}} e_k(\alpha),$$

with

$$e_k(\alpha) = A||u_{0,k} - u_{2,k}||^2_{L_2(]-L,0[)} + B||\nabla(u_{0,k} - u_{2,k})||^2_{L_2(]-L,0[)},$$

where we have decomposed decomposed u_0, u_1 and u_2 into modes in the y direction, denoting by k the associated wave number.

The mode $u_{0,k}$ solves

$$\partial_{xx} u_{0,k} - \left(k^2 - \frac{\xi_0}{\mu_0}\omega^2\right) u_{0,k} = 0,$$

and thus

$$u_{0,k}(x) = A_0 \exp(\lambda_0 x) + B_0 \exp(-\lambda_0 x), \tag{43}$$

where λ_0 is given in Eq. (42).

The mode $u_{1,k}$ solves

$$\partial_{xx} u_{1,k} - \left(k^2 - \frac{\tilde{\xi}_1}{\mu_1}\omega^2\right) u_{1,k} = 0,$$

and thus

$$u_{1,k}(x) = A_1 \exp(\lambda_1 x) + B_1 \exp(-\lambda_1 x), \tag{44}$$

where

$$\lambda_1^2 = k^2 - \left(1 + \frac{ai}{\xi_1\omega}\right)\frac{\xi_1}{\mu_1}\omega^2,$$

so that

$$\lambda_1 = \frac{1}{\sqrt{2}}\sqrt{k^2 - \frac{\xi_1}{\mu_1}\omega^2 + \sqrt{\left(k^2 - \frac{\xi_1}{\mu_1}\omega^2\right)^2 + \left(\frac{a\omega}{\mu_1}\right)^2}}$$
$$-\frac{i}{\sqrt{2}}\sqrt{\frac{\xi_1}{\mu_1}\omega^2 - k^2 + \sqrt{\left(k^2 - \frac{\xi_1}{\mu_1}\omega^2\right)^2 + \left(\frac{a\omega}{\mu_1}\right)^2}}.$$

For large L, since $Re(\lambda_1) > 0$, the value of A_1 tend to 0, so that we may neglect the first contribution in the right-hand side of (44). Consequently we consider the expression

$$u_{1,k}(x) = B_1 \exp(-\lambda_1 x). \tag{45}$$

Continuity conditions (37) and expressions (43) and (45) imply the following relations

$$A_0 + B_0 = B_1 \quad , \quad \mu_0\lambda_0(A_0 - B_0) = -\mu_1\lambda_1 B_1,$$

from which we infer that

$$B_0 = \frac{\lambda_0\mu_0 + \lambda_1\mu_1}{\lambda_0\mu_0 - \lambda_1\mu_1} A_0,$$

and thus

$$u_{0,k}(x) = A_0\left[\exp(\lambda_0 x) + \frac{\lambda_0\mu_0 + \lambda_1\mu_1}{\lambda_0\mu_0 - \lambda_1\mu_1}\exp(-\lambda_0 x)\right].$$

The decomposition of the boundary condition (38) into Fourier modes implies that $u_{0,k}(-L) = g_k$, which gives the final expression

$$u_{0,k}(x) = g_k \frac{[(\lambda_0\mu_0 - \lambda_1\mu_1)\exp(\lambda_0 x) + (\lambda_0\mu_0 + \lambda_1\mu_1)\exp(-\lambda_0 x)]}{[(\lambda_0\mu_0 - \lambda_1\mu_1)\exp(-\lambda_0 L) + (\lambda_0\mu_0 + \lambda_1\mu_1)\exp(\lambda_0 L)]}. \tag{46}$$

Let us now turn to the expression of $u_{2,k}$. Since equation (39) is the same as that verified by $u_{0,k}$, both solutions have the same general form:

$$u_{2,k}(x) = A_2 \exp(\lambda_0 x) + B_2 \exp(-\lambda_0 x).$$

The Robin boundary condition (40) on Γ implies that

$$\mu_0\lambda_0(A_2 - B_2) + \alpha(A_2 + B_2) = 0,$$

which means that

$$u_{2,k}(x) = A_2\left[\exp(\lambda_0 x) + \frac{\lambda_0\mu_0 + \alpha}{\lambda_0\mu_0 - \alpha}\exp(-\lambda_0 x)\right].$$

Application of the boundary condition (41) implies the final expression

$$u_{2,k}(x) = g_k\frac{[(\lambda_0\mu_0 - \alpha)\exp(\lambda_0 x) + (\lambda_0\mu_0 + \alpha)\exp(-\lambda_0 x)]}{[(\lambda_0\mu_0 - \alpha)\exp(-\lambda_0 L) + (\lambda_0\mu_0 + \alpha)\exp(\lambda_0 L)]}. \tag{47}$$

Using (46) and (47), we have that

$$(u_{0,k} - u_{2,k})(x) = \chi(k,\alpha)\exp(\lambda_0 x) + \eta(k,\alpha)\exp(-\lambda_0 x), \tag{48}$$

where the coefficients χ and η are computed from (46) and (47). In order to compute the L_2 norm of this expression, we must first compute the square of its modulus (by $\bar{\eta}$ is denoted the complex conjugate of η):

$$|u_{0,k} - u_{2,k}|^2(x) = |\chi|^2|\exp(\lambda_0 x)|^2 + |\eta|^2|\exp(-\lambda_0 x)|^2 + 2\mathrm{Re}\left(\chi\bar{\eta}\exp(\lambda_0 x)\overline{\exp(-\lambda_0 x)}\right).$$

Note that, according to the values of k, the expression above may be simplified into

$$|u_{0,k} - u_{2,k}|^2(x) = |\chi|^2\exp(2\lambda_0 x) + |\eta|^2\exp(-2\lambda_0 x) + 2\mathrm{Re}\left(\chi\bar{\eta}\right),$$

if $k^2 \geq \frac{\xi_0}{\mu_0}\omega^2$, or

$$|u_{0,k} - u_{2,k}|^2(x) = |\chi|^2 + |\eta|^2 + 2\mathrm{Re}\left(\chi\bar{\eta}\exp(2\lambda_0 x)\right),$$

if $k^2 < \frac{\xi_0}{\mu_0}\omega^2$. Thus, we have for $k^2 \geq \frac{\xi_0}{\mu_0}\omega^2$

$$\begin{aligned}\int_{-L}^{0}|u_{0,k} - u_{2,k}|^2(x)\mathrm{d}x = \ & \tfrac{1}{2\lambda_0}\left\{|\chi|^2\left[1 - \exp(-2\lambda_0 L)\right] + |\eta|^2\left[\exp(2\lambda_0 L) - 1\right]\right\} \\ & + 2L\mathrm{Re}\left(\chi\bar{\eta}\right)\end{aligned}$$

or, for $k^2 < \frac{\xi_0}{\mu_0}\omega^2$,

$$\int_{-L}^{0}|u_{0,k} - u_{2,k}|^2(x)\mathrm{d}x = L(|\chi|^2 + |\eta|^2) + \frac{i}{\lambda_0}\mathrm{Im}\left\{\chi\bar{\eta}\left[1 - \exp(-2\lambda_0 L)\right]\right\}.$$

Now, we also have to compute the L_2 norm of the gradient of $(u_{0,k} - u_{2,k})$. Noting that

$$\nabla(u_{0,k} - u_{2,k}) = \begin{pmatrix} \partial_x(u_{0,k} - u_{2,k}) \\ ik(u_{0,k} - u_{2,k}) \end{pmatrix},$$

it holds that

$$|\nabla(u_{0,k} - u_{2,k})|^2 = |k|^2|u_{0,k} - u_{2,k}|^2 + |\partial_x(u_{0,k} - u_{2,k})|^2.$$

With expression (48), it follows that

$$|\partial_x(u_{0,k} - u_{2,k})|^2 = |\lambda_0|^2\left[|\chi|^2\exp(2\lambda_0 x) + |\eta|^2\exp(-2\lambda_0 x) - 2\mathrm{Re}\left(\chi\bar{\eta}\right)\right],$$

if $k^2 \geq \frac{\xi_0}{\mu_0}\omega^2$, or

$$|\partial_x(u_{0,k} - u_{2,k})|^2 = |\lambda_0|^2\left[|\chi|^2 + |\eta|^2 - 2\mathrm{Re}\left(\chi\bar{\eta}\exp(2\lambda_0 x)\right)\right],$$

if $k^2 < \frac{\xi_0}{\mu_0}\omega^2$, and thus

$$\int_{-L}^{0} |\partial_x(u_{0,k} - u_{2,k})|^2(x)\mathrm{d}x = \frac{\lambda_0}{2}\left\{|\chi|^2\left[1-\exp(-2\lambda_0 L)\right] + |\eta|^2\left[\exp(2\lambda_0 L) - 1\right]\right\} - 2\lambda_0^2 L\mathrm{Re}\left(\chi\bar{\eta}\right),$$

if $k^2 \geq \frac{\xi_0}{\mu_0}\omega^2$, or, if $k^2 < \frac{\xi_0}{\mu_0}\omega^2$,

$$\int_{-L}^{0} |\partial_x(u_{0,k} - u_{2,k})|^2(x)\mathrm{d}x = L|\lambda_0|^2\left(|\chi|^2 + |\eta|^2\right) + i\lambda_0\mathrm{Im}\left\{\chi\bar{\eta}\left[1-\exp(-2\lambda_0 L)\right]\right\}.$$

Therefore, we can find α as the solution of the mentioned minimization problem. □

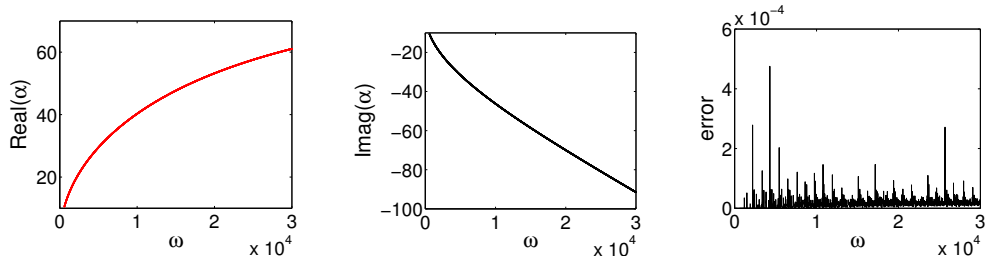

(a) Re(α) (b) Im(α) (c) error

Figure 11: The real (top left) and imaginary (top right) parts of α and the sum of the errors $e_{\Delta x}$ (in the bottom) as function of frequencies $\omega \in [600, 30000]$ calculated for the ISOREL porous material.

Since the minimization will be done numerically and since the sequence $(z, -z, z - z, \cdots) = z(\exp(i(j\Delta x)/\Delta x))$ is the highest frequency mode that can be reached on a grid of size Δx, then, in practice, the sum may be truncated to

$$e_{\Delta x}(\alpha) := \sum_{k=\frac{n\pi}{L}, n\in\mathbb{Z}, -\frac{L}{\Delta x}\leq n\leq\frac{L}{\Delta x}} e_k(\alpha).$$

For the equations (35)–(36), we use the same coefficients as for problem (1) and take the values corresponding to a porous medium, called ISOREL, using in the building isolation. More precisely we assume: $\phi = 0.7$, $\gamma_p = 1.4$, $\sigma = 142300N.m^{-4}.s$, $\rho_0 = 1.2kg/m^3$, $\alpha_h = 1.15$, $c_0 = 340m.s^{-1}$. We could find the value of α presented in Figure 11.

Remark 2. *Figure 11 allows us to compare the difference between two considered time-dependent models for the damping in the volume and for the damping on the boundary. We see that* $\mathrm{Re}(\alpha)$ *is not a constant in general, but for* $\omega \to +\infty$ $\mathrm{Im}(\alpha)$ *is a linear function of* ω*. In this sense, the damping properties of two models are almost the same, but the reflection is more accurately considered by the damping wave equation in the volume.*

References

[1] K. Abe, T. Fujiu, and K. Koro. A BE-based shape optimization method enhanced by topological derivative for sound scattering problems. *Engineering Analysis with Boundary Elements*, 34(12):1082–1091, Dec 2010.

[2] Y. Achdou and O. Pironneau. Optimization of a photocell. *Optimal Control Applications and Methods*, 12(4):221–246, Oct 1991.

[3] S. Agmon. *Lectures on elliptic boundary value problems*. Van Mostrand Math. Studies, 1965.

[4] G. Allaire. *Conception optimale de structures*. 58 Mathématiques et Applications, Springer, 2007.

[5] H. Antil, S. Hardesty, and M. Heinkenschloss. Shape Optimization of Shell Structure Acoustics. *SIAM Journal on Control and Optimization*, 55(3):1347–1376, Jan 2017.

[6] K. Arfi and A. Rozanova Pierrat. Dirichlet-to-Neumann or Poincaré-Steklov operator on fractals described by d-sets. *Discrete and Continuous Dynamical Systems - S*, 12:1–26, 2019.

[7] M. Asch and G. Lebeau. The Spectrum of the Damped Wave Operator for a Bounded Domain in $\mathbb{R}^2$. *Experimental Mathematics*, 12(2):227–241, Jan 2003.

[8] C. Bardos and J. Rauch. Variational algorithms for the Helmholtz equation using time evolution and artificial boundaries. *Asymptotic Analysis*, 9:101–117, 1994.

[9] D. Bucur, D. Mazzoleni, A. Pratelli, and B. Velichkov. Lipschitz Regularity of the Eigenfunctions on Optimal Domains. *Arch Rational Mech Anal*, 216(1):117–151, Oct 2014.

[10] Y. Cao and D. Stanescu. Shape optimization for noise radiation problems. *Computers & Mathematics with Applications*, 44(12):1527–1537, Dec 2002.

[11] R. Capitanelli. Asymptotics for mixed Dirichlet–Robin problems in irregular domains. *Journal of Mathematical Analysis and Applications*, 362(2):450–459, Feb 2010.

[12] R. Capitanelli. Robin boundary condition on scale irregular fractals. *Communications on Pure and Applied Analysis*, 9(5):1221–1234, May 2010.

[13] D. Chenais. On the existence of a solution in a domain identification problem. *Journal of Mathematical Analysis and Applications*, 52(2):189–219, Nov 1975.

[14] S. Cox and E. Zuazua. The rate at which energy decays in a damped string. *Communications in Partial Differential Equations*, 19(1-2):213–243, Jan 1994.

[15] S. Creo, M. R. Lancia, P. Vernole, M. Hinz, and A. Teplyaev. Magnetostatic problems in fractal domains. 2018.

[16] J. Dardé. *Méthodes de quasi-réversibilité et de lignes de niveau appliquées aux problèmes inverses elliptiques*. PhD thesis, 2010.

[17] A. Dekkers. *Mathematical analysis of the Kuznetsov equation : Cauchy problem, approximation questions and problems with fractals boundaries*. PhD thesis, 2019.

[18] D. Duhamel. *Calcul de murs antibruit et control actif du son*. PhD thesis, 1998.

[19] D. Duhamel. Shape optimization of noise barriers using genetic algorithms. *Journal of Sound and Vibration*, 297(1-2):432–443, Oct 2006.

[20] L. C. Evans. *Partial Differential Equations*. American Math Society, 2010.

[21] B. Farhadinia. An Optimal Shape Design Problem for Fan Noise Reduction. *JSEA*, 03(06):610–613, 2010.

[22] S. Félix, M. Asch, M. Filoche, and B. Sapoval. Localization and increased damping in irregular acoustic cavities. *Journal of Sound and Vibration*, 299(4-5):965–976, Feb 2007.

[23] M. J. Gander, L. Halpern, and F. Magoulès. An optimized Schwarz method with two-sided Robin transmission conditions for the Helmholtz equation. *International Journal for Numerical Methods in Fluids*, 55(2):163–175, 2007.

[24] A. GIROUARD, L. PARNOVSKI, I. POLTEROVICH, and D. A. SHER. The Steklov spectrum of surfaces: asymptotics and invariants. *Mathematical Proceedings of the Cambridge Philosophical Society*, 157(03):379–389, Aug 2014.

[25] C. Gordon, P. Herbrich, and D. Webb. Robin and Steklov isospectral manifolds. *preprint*, 2015.

[26] C. Gordon, P. Perry, and D. Schueth. Isospectral and isoscattering manifolds: a survey of techniques and examples. *Geometry, spectral theory, groups, and dynamics, Contemp. Math.*, 387:157–179, 2005.

[27] D. Guicking. On the invention of active noise control by Paul Lueg. *The Journal of the Acoustical Society of America*, 87(5):2251, 1990.

[28] P. Hajłasz, P. Koskela, and H. Tuominen. Sobolev embeddings, extensions and measure density condition. *Journal of Functional Analysis*, 254(5):1217–1234, Mar 2008.

[29] J.-F. Hamet and M. Berengier. Acoustical characteristics of porous pavements: a new phenomenological model. *Internoise 93,Louvain, Belgique*, pages 641–646, 1993.

[30] A. Henrot and M. Pierre. *Variation et optimization de formes. Une analyse géométrique.* Springer, 2005.

[31] A. Jonsson and H. Wallin. *Function spaces on subsets of* $\mathbb{R}^n$. Math. Reports 2, Part 1, Harwood Acad. Publ. London, 1984.

[32] A. Jonsson and H. Wallin. The dual of Besov spaces on fractals. *Studia Mathematica*, 112(3):285–300, 1995.

[33] A. Jonsson and H. Wallin. Boundary value problems and brownian motion on fractals. *Chaos, Solitons & Fractals*, 8(2):191–205, Feb 1997.

[34] M. R. Lancia. A Transmission Problem with a Fractal Interface. *Zeitschrift für Analysis und ihre Anwendungen*, 21(1):113–133, 2002.

[35] J. Lions and E. Magenes. *Non-Homogeneous Boundary Value Problems and Applications*, volume 1. Berlin: Springer-Verlag, 1972.

[36] J. Marschall. The trace of Sobolev-Slobodeckij spaces on Lipschitz domains. *Manuscripta Math*, 58(1-2):47–65, Mar 1987.

[37] V. Maz'ja. *Sobolev Spaces.* Springer Ser. Sov. Math., Springer-Verlag, Berlin,, 1985.

[38] B. Mohammadi and O. Pironneau. *Applied shape optimization for fluids.* Oxford University Press, 2010.

[39] A. Münch. Optimal Internal Dissipation of a Damped Wave Equation Using a Topological Approach. *International Journal of Applied Mathematics and Computer Science*, 19(1), Jan 2009.

[40] A. Münch, P. Pedregal, and F. Periago. Optimal design of the damping set for the stabilization of the wave equation. *Journal of Differential Equations*, 231(1):331–358, Dec 2006.

[41] S. Osher and R. Fedkiw. *Level set method and dynamic implicit surfaces*, volume 153. Applied Mathematical Sciences, Springer, 2003.

[42] S. Osher and J.-A. Sethian. Fronts propagating with curvature dependent speed: algorithm based on Hamilton-Jacobi formulations. *J. Comp. Phys*, 79, 1988.

[43] J. Sethian and R. Fedkiw. *Level set method and fast marching methods.* Cambridge Univerity Press, 1999.

[44] H. Wallin. The trace to the boundary of Sobolev spaces on a snowflake. *Manuscripta Math*, 73(1):117–125, Dec 1991.